INT. REVIEWS IN PHYSICAL CHEMISTRY, 2000, VOL. 19, NO. 4. 565–607

Cavity ring-down spectroscopy: Experimental schemes and applications

GIEL BERDEN†, RUDY PEETERS† and GERARD MEIJER†‡

† Department of Molecular and Laser Physics, Toernooiveld 1, 6525 ED Nijmegen, The Netherlands

‡ FOM Institute for Plasma Physics Rijnhuizen, Edisonbaan 14, 3439 MN Nieuwegein, The Netherlands

Cavity ring-down (CRD) spectroscopy is a direct absorption technique, which can be performed with pulsed or continuous light sources and has a significantly higher sensitivity than obtainable in conventional absorption spectroscopy. The CRD technique is based upon the measurement of the rate of absorption rather than the magnitude of absorption of a light pulse confined in a closed optical cavity with a high Q factor. The advantage over normal absorption spectroscopy results from, firstly, the intrinsic insensitivity to light source intensity fluctuations and, secondly, the extremely long effective path lengths (many kilometres) that can be realized in stable optical cavities. In the last decade, it has been shown that the CRD technique is especially powerful in gas-phase spectroscopy for measurements of either strong absorptions of species present in trace amounts or weak absorptions of abundant species. In this review, we emphasize the various experimental schemes of CRD spectroscopy, and we show how these schemes can be used to obtain spectroscopic information on atoms, molecules, ions and clusters in many environments such as open air, static gas cells, supersonic expansions, flames and discharges.

Contents

International Reviews in Physical Chemistry ISSN 0144-235X print/ISSN 1366-591X online
http://www.tandf.co.uk/journals

1. Introduction

Direct absorption spectroscopy of atoms and molecules in the gas phase, yielding both quantitative absolute concentrations as well as absolute frequency-dependent cross-sections, is a very powerful tool in analytical chemistry and physical chemistry. This absoluteness is the reason why sensitive absorption spectroscopy techniques have gained renewed interest, even in research fields where more sophisticated laser-based diagnostic techniques are commonly applied. Among the various direct absorption techniques, the cavity ring-down (CRD) technique has proven to be a valuable addition, since it combines a good sensitivity with a rather simple and straightforward experimental set-up.

In a 'conventional' absorption experiment, one measures the amount of light that is transmitted through a sample. If the light source is monochromatic (e.g. a laser), one can record an absorption spectrum of the sample by recording the transmitted intensity as a function of the frequency. Alternatively, a broad light source can be used when the incident light or the transmitted light is spectrally dispersed. A drawback of direct absorption might be its limited sensitivity. A small attenuation in transmitted light has to be measured on top of a large background. High sensitivity is obtained by using modulation schemes and by increasing the absorption path length. Alternatively, other experimental spectroscopy techniques can be used which are based on the detection of phenomena which are induced by absorption of light, such as pressure changes in photoacoustic spectroscopy, fluorescence in laser-induced fluorescence (LIF), or ions in resonant enhanced multiphoton ionization (REMPI). The great advantage of these techniques is that they are background free. A disadvantage is the sometimes difficult calibration procedure which is needed to make these techniques absolute (i.e. these techniques are not self-calibrating).

CRD spectroscopy is a sensitive absorption technique in which the rate of absorption rather than the magnitude of the absorption of a light pulse confined in an optical cavity is measured. The sample is placed inside a high-finesse optical cavity consisting of two highly reflective mirrors. A short laser pulse is coupled into the cavity, the light is reflected back and forth inside the cavity and, every time that the light is reflected, a small fraction of this light leaks out of the cavity. Instead of measuring the total intensity of the light exiting the cavity, one determines the decay time by measuring the time dependence of the light leaking out of the cavity. In this way the rate of absorption can be obtained; the more the sample absorbs, the shorter is the measured decay time. There are several advantages to this approach. Since the absorption is determined from the time behaviour of the signal, it is independent of pulse-to-pulse fluctuations of the laser. Furthermore, the effective absorption path length, which depends on the reflectivity of the cavity mirrors, can be very long (up to several kilometres), while the sample volume can be kept rather small. Compared with other sensitive absorption techniques, especially those using modulation schemes, CRD spectroscopy has the additional advantage that the absorption is measured on an absolute scale. Another attractive property is its simplicity, it is rather easy to construct a CRD set-up out of a few components.

The work reported by Herbelin *et al.* (1980) and Anderson *et al.* (1984) can be regarded as precursors to the CRD technique, although the transmission of a light

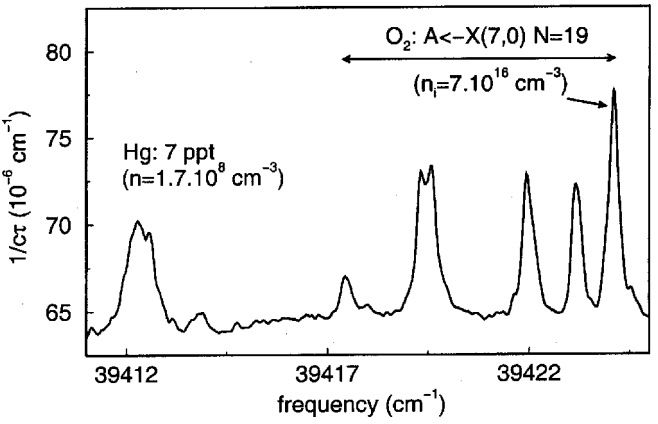

Figure 1. CRD absorption spectrum of ambient air around 253·7 nm measured in a cavity 45 cm long, using mirrors with a reflection coefficient of only 99·7%. It demonstrates the use of CRD spectroscopy for trace gas detection (atomic mercury; with the known cross-section for this transition the density of these atoms can be determined) and for measuring absolute cross-sections (molecular oxygen; with the known density the cross-section can be determined). (Figure reproduced from Jongma *et al.* (1995) with permission. Copyright the American Institute of Physics).

pulse through an optical cavity has already been studied for a long time (see for example Kastler (1974)). Herbelin *et al.* (1980) were the first to propose the use of an optical cavity for measuring the reflectance of mirror coatings (the reflection losses are, in a way, the 'absorption' of the optical cavity). By intensity modulating a continuous-wave (CW) light beam and measuring the phase shift introduced by the optical cavity, they were able to determine accurately the high reflectance of their mirrors. In 1984, Anderson *et al.* demonstrated that the reflectance could be measured even better by abruptly switching off the CW light source when the intracavity field exceeded a certain threshold value, followed by a recording of the subsequent intensity decay of the light in the optical cavity. In both techniques, injection of light into the cavity occurred via accidental coincidences of the (narrow-bandwidth) laser frequency with the frequency of one of the narrow cavity modes.

In 1988 O'Keefe and Deacon showed that problems associated with mode coincidences could be circumvented by using a pulsed laser. Additionally, owing to the pulsed character, no electronics were needed for monitoring the intracavity power or for switching off the laser, before observing the decay transient, thus providing a simple experimental design for measuring the cavity loss. O'Keefe and Deacon realized that this method was suitable for measuring the absorption spectrum of molecules present in the cavity. They demonstrated the sensitivity by recording the CRD absorption spectrum of the weak $b\,^1\Sigma_g^+(v = 1, 2) \leftarrow X\,^3\Sigma_g^-(v = 0)$ bands of molecular oxygen (O'Keefe and Deacon 1988). Since then, it has been shown by many groups that this technique is powerful in gas-phase spectroscopy for measurements of either strong absorptions of species present in trace amounts or weak absorptions of abundant species (figure 1).

Although CRD spectroscopy is significantly more sensitive than 'conventional' absorption spectroscopy, in general it cannot compete with background-free detection techniques such as LIF or REMPI. The CRD technique, however, can still be applied with success when the molecule's excited state does not fluoresce (a prerequisite for

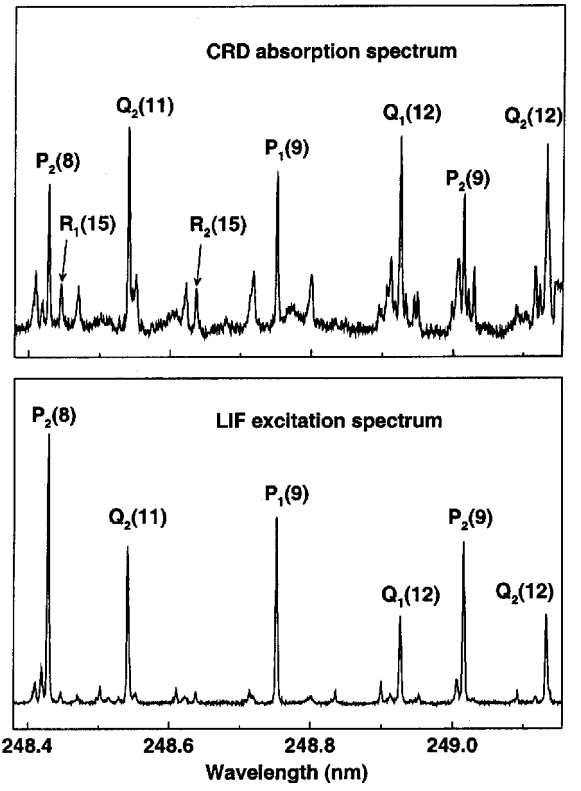

Figure 2. Part of the $A\,^2\Sigma^+(v' = 3) \leftarrow X\,^2\Pi(v'' = 0)$ spectrum of OH, measured simultaneously by CRD and LIF spectroscopy in a laminar methane–air flame at atmospheric pressure. The differences in relative intensity are due to the rotational dependence on the predissociation rate; with increasing rotational quantum number in the $A\,^2\Sigma^+(v' = 3)$ state, the predissociation rate increases. (Figure reproduced from Spaanjaars *et al*. (1997) with permission. Copyright the American Institute of Physics).

LIF) or cannot be ionized (a prerequisite for REMPI). In high-pressure samples, such as flames and plasmas, CRD can be successfully used to extract quantitative absolute concentration data, which is nearly impossible by either LIF (because of difficulties associated with collisional quenching of the fluorescing state (figure 2)) or by REMPI (owing to difficulties in extracting the charged particles).

To date, the CRD technique has been successfully applied in various environments. High resolution spectroscopy studies have been performed on molecules in cells and supersonic jets and on transient molecules generated in discharges, flow reactors and flames. The CRD spectra directly provide the frequency-dependent absorption strengths of the molecules under study, which contain information on the number density, cross-section and temperature. As long as mirrors with a sufficiently high reflectivity, detectors with a sufficiently fast time response, and tunable (pulsed) light sources are available, there is no intrinsic limitation to the spectral region in which CRD can be applied. By now, successful application of CRD spectroscopy has been demonstrated from the ultraviolet (UV) part of the spectrum to the infrared (IR) spectral region.

Although nowadays most CRD experiments are performed with pulsed lasers, several schemes have been developed during the last 5 years in order to perform CRD

spectroscopy with CW lasers. Advantages of continuous-wave cavity ring-down spectroscopy (CW-CRD) are a better spectral resolution and a better duty cycle. Furthermore, the sensitivity of CW-CRD can in principle be improved by careful design of the coupling of the laser modes to the cavity modes. It is interesting to note that the first two CW-CRD experiments which have been reported are inspired by the aforementioned 'precursor' experiments. Engeln *et al*. (1996) reported phase-shift cavity ring-down (PS-CRD) spectroscopy, in which the absorption spectrum is extracted from a measurement of the magnitude of the phase shift that an intensity-modulated CW light beam experiences upon passage through an optical cavity. Later, Romanini *et al*. (1997a) used the other approach; the resonant cavity mode is swept over the CW laser line; then, when sufficient light is coupled into the cavity, the laser is switched off; subsequently, the CRD transient is recorded.

Several review papers on CRD spectroscopy exist. An historical overview of the development of CRD spectroscopy can be found in the book edited by Busch and Busch (1999). This book contains also papers on the theory of optical cavities, different CRD techniques and applications of CRD spectroscopy. Scherer *et al*. (1995d, 1997b) and Paul and Saykally (1997) have reviewed the early literature and the application of CRD spectroscopy to pulsed molecular beams. An overview of the use of CRD spectroscopy for the study of fast (subnanosecond) predissociation of electronically excited states of small molecules and radicals has been given by Wheeler *et al*. (1998c). Cheskis (1999) discussed the application of the CRD technique to the measurements of radicals in flames. Applications in analytical atomic spectroscopy have been reviewed by Miller and Winstead (2000).

In this article, we emphasize the various experimental schemes of CRD spectroscopy and their applications. First, we outline the basic concepts of 'conventional' pulsed CRD spectroscopy, and we show that the CRD technique can be combined with other spectroscopic techniques such as Fourier transform (FT) spectroscopy and magnetic rotation spectroscopy (MRS). Then we shall discuss the development of CW-CRD spectroscopy and make the step to cavity-enhanced absorption (CEA) spectroscopy. The latter technique, which has been developed recently, is a simple CW absorption technique which uses ideas from the field of CRD spectroscopy. We illustrate all these techniques with some key studies in order to try to convince the reader that CRD spectroscopy is indeed a powerful technique.

2. Pulsed cavity ring-down spectroscopy

2.1. *Principle*

In a typical CRD experiment, a light pulse with a spectral intensity distribution $I(\nu)$ and a duration which is shorter than the 'CRD time' τ (defined below) is coupled into a non-confocal optical cavity consisting of two highly reflecting mirrors. The fraction of the light that is successfully coupled into the cavity bounces back and forth between the mirrors. The intensity of the light inside the cavity decays as a function of time, since at each reflection of a mirror a small fraction of the light is coupled out of the cavity. The time dependence of the intensity inside the cavity is easily monitored by measuring the intensity of the light exiting the cavity.

In an empty cavity, this ring-down transient is a single-exponentially decaying function of time with a 1/e CRD time $\tau(\nu)$ which is solely determined by the reflectivity $R(\nu)$ of the mirrors and the optical path length d between the mirrors. The presence of absorbing species in the cavity gives an additional loss channel for the light inside the cavity. If the absorption follows Beer's law, the light intensity inside the cavity will still

decay exponentially, resulting in a decrease in the CRD time τ. Generally, the intensity of the light exiting the cavity is given by

$$I_{\mathrm{CRD}}(t) \propto \int_0^{\infty} I(\nu) \exp\left[-\frac{t}{\tau(\nu)}\right] \mathrm{d}\nu, \tag{1}$$

where the ring-down time is given by

$$\tau(\nu) = \frac{d}{c\{|\ln[R(\nu)]| + \Sigma_i \sigma_i(\nu) \int_0^l N_i(x)\,\mathrm{d}x\}}, \tag{2}$$

where c is the speed of light and the sum is over all light-scattering and light-absorbing species with frequency-dependent cross-sections $\sigma_i(\nu)$ and a line-integrated number density $\int_0^l N_i(x)\mathrm{d}x$ (in the case when the complete cavity is filled with absorbing or scattering species, l will be equal to d). When considering narrow frequency intervals the frequency dependence of the Rayleigh cross-section $\sigma_{\mathrm{Ray}}(\nu)$ and the Mie cross-section $\sigma_{\mathrm{Mie}}(\nu)$ as well as of the mirror reflectivity can be neglected, and an effective loss factor $|\ln(R_{\mathrm{eff}})|$ is taken. This effective loss factor may also include broad-band absorption. The product of the absorption cross-section $\sigma_{\mathrm{i}}(\nu)$ and the number density $N_i(x)$ is commonly expressed as the absorption coefficient $\kappa_i(\nu, x)$ (also frequently denoted as $\alpha_i(\nu, x)$).

The reflectivity of the mirrors is typically $R = 0.99$ or better. Since the contributions of broad-band scattering and absorption to R_{eff} are generally much smaller than the reflection losses of the mirrors and $R \approx 1$, one can write $|\ln(R_{\mathrm{eff}})| \approx 1 - R_{\mathrm{eff}}$. If we take the special case in which the number density does not depend on the position inside the cavity, equation (2) can be written in a form which is often used in the CRD literature:

$$\tau(\nu) = \frac{d}{c[(1-R) + \kappa(\nu) l]}, \tag{3}$$

where we have replaced R_{eff} by R just for convenience. The ringdown time depends only on the properties of the cavity and the absorbing species present in the cavity and is independent of the amplitude of the light inside the cavity.

In a CRD experiment the CRD time τ is measured as a function of the laser frequency ν. An absorption spectrum is obtained by plotting the cavity loss $1/c\tau$ as a function of ν. The background in this spectrum is then given by $(1-R)/d$. Absolute absorption strengths can thus be obtained by subtracting the off-resonance cavity loss from the on-resonance cavity loss.

2.2. *Experimental set-up*

There are no intrinsic limitations to the spectral region in which CRD can be applied, provided that mirrors with a sufficiently high reflectivity, detectors with a sufficiently fast time response, and tuneable pulsed lasers are available. A typical experimental CRD set-up is given in figure 3. This basic set-up is fairly simple; it consists of a pulsed laser system, a ring-down cavity, a fast detector, a fast and deep analogue-to-digital converter, and a computer for data handling. The actual choice of these components depends on the wavelength region in which the CRD spectrum needs to be recorded.

In the visible wavelength region, CRD spectroscopy is usually performed with pulsed dye lasers (typical pulse duration of 5–15 ns). Only moderate pulse energies

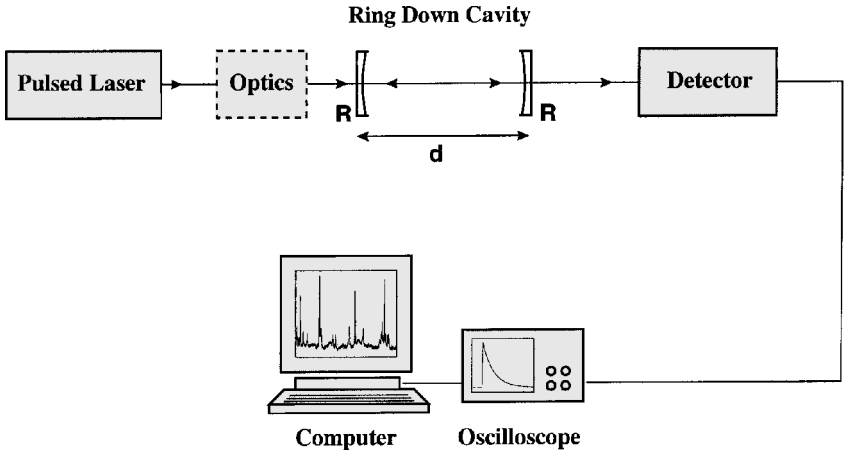

Figure 3. Scheme of the experimental set-up for CRD spectroscopy. The mode-matching optics are optional (see text).

(~ 1 mJ) are needed. In this wavelength region, highly reflective mirrors are available ($1-R$ from 10^{-3} down to 10^{-6}), and time-dependent detection of the light leaking out of the ring-down cavity is easily performed with a photomultiplier tube (PMT). Tuneable pulsed UV light can be generated by, for example, frequency doubling or Raman-shifting visible laser light. The reflectivity of the ring-down mirrors is somewhat worse compared with the reflectivity available in the visible spectral region ($1-R \approx 10^{-2}$–10^{-3}). Again a PMT can be used as a detector. Tuneable pulsed IR light can be obtained by Raman shifting or frequency mixing visible laser light, or by using for example an optical parametric oscillator (OPO), a CO_2 laser or a free-electron laser. The reflectivity of the mirrors in the near IR is comparable with that in the visible region but becomes worse when going to the far-IR (typical losses are 10^{-3} at around 10 μm). The ring-down transients can be recorded with liquid nitrogen cooled HgCdTe detectors.

The ring-down cavity is formed by two identical plano-concave mirrors. The radius of curvature r is typically between -25 cm and -1 m, and the mirrors are placed at a distance d such that the cavity is optically stable (and non-confocal), that is $0 < d < r$ or $r < d < 2r$. Cavity lengths of 3 cm (see section 2.6.1) (Berden *et al.* 1998) up to 270 cm (Le Grand and Le Floch 1990) have been reported. The mirrors are placed in mounts such that their positions can be adjusted in order to align the cavity. For cell experiments the mounts are connected to a tube in such a way that the mirrors act as entrance and exit windows of the cell. It is very difficult ('impossible') to place a cell *inside* a cavity since the reflection and absorption losses of the cell windows are too large for observing a CRD transient (although experiments have been performed with optical elements inside the cavity, see section 2.7).

Suppose that we have mirrors with a reflectivity of 0.9999 and a radius of curvature of -1 m placed at a distance of 0.5 m. The effective path length $d/(1-R)$ is then equal to 5000 m, and the decay time τ is 16.7 μs. An absorption $\kappa = 10^{-8}$ cm^{-1} changes the decay time to 16.6 μs. In order to observe this absorption it is important to determine the decay time accurately. Obviously, the most accurate way is to use a digitizer with the highest vertical resolution (10 bits or higher) and horizontal resolution (20 Ms s^{-1} or higher). In our laboratory we use a fast (100 Ms s^{-1}) digital oscilloscope with a 10

bit vertical resolution (Le Croy 9430). The decay transient is recorded over three or four times the decay time of the empty cavity. After averaging the ring-down transients over a predefined number of laser pulses (20–50) on the on-board memory of the oscilloscope, the data are transferred to a personal computer (PC). After subtracting the baseline of the data, the natural logarithm of the data is taken and the result is fitted to a straight line using a least-squares weighted fitting algorithm. The slope of this fitted line is recorded as a function of the laser frequency.

Instead of recording the complete ring-down transient, Romanini and Lehmann (1993) used two boxcar channels which integrate and average the decay inside two time windows. The natural logarithm of the ratio of the signals measured at both channels is then proportional to the absorption coefficient. O'Keefe (1998) used two unequal time windows. The first gate integrates the complete decay transient, providing a signal which is proportional to the laser pulse energy and the ring-down time τ, while the second gate measures the laser pulse energy from the very first part of the decay transient. The ratio of the two signals provides the ring-down time τ.

2.3. *Cavity modes*

Above, we have given a rather simplified picture of CRD spectroscopy, namely a pulse of light which is reflected back and forth in a high-finesse optical cavity. This picture gives the impression that this process is independent of the frequency of the laser light exciting the cavity, which is obviously not the case since we have to consider the mode structure of the cavity. This mode structure can cause several problems. Narrow molecular absorption features might fall between the cavity modes and these features will then be absent in the spectrum. Furthermore, mode beating, resulting from multimode excitation, can generate oscillations in the ring-down transient, which prevents an accurate determination of the decay time τ.

Potential problems associated with the mode structure can easily be cirvumvented by using a stable optical cavity with a near-continuum mode structure (Meijer *et al.* 1994, Engeln *et al.* 1996). In general, a cavity has both longitudinal and transverse modes. The frequency of a TEM_{qmn} mode having a longitudinal index q and transverse indices m, n is given by (see for example Hodges *et al.* (1996b))

$$\nu_{qmn} = \frac{c}{2d}\left[q+(m+n+1)\frac{2}{\pi}\arctan\left(\frac{d}{[d(2r-d)]^{1/2}}\right)\right]. \tag{4}$$

From this equation it is seen that the longitudinal mode spacing (often referred to as the free spectral range of the cavity) is $\Delta\nu = c/2d$ and that the transverse mode spacing is given by $(c/\pi d)\arctan\{d/[d(2r-d)]^{1/2}\}$. Therefore, the mode structure in the cavity is a continuum when the ratio of the transverse to longitudinal mode spacings is irrational.

Experimentally, such a continuum can readily be achieved. First of all, no mode-matching optics should be used to couple light into the cavity. Second, the cavity should be stable (and non-confocal), that is $0 < d < r$ or $r < d < 2r$. Third, the ratio of the mirror diameter to the length of the cavity should be not too small in order to ensure that the transverse modes remain in the cavity (i.e. the diffraction losses of the transverse modes should be minimized). Finally, care should be taken that all modes exiting the cavity are detected with equal efficiency, since transverse modes are spatially more extended. For example, a cavity with a length of 50 cm, mirrors with a diameter of 25 mm, and a radius r of curvature of -1 m satisfies the second and third

conditions. All modes are detected by placing a photomultiplier directly behind the cavity. If the effective surface of the detector is small, a lens with an appropriate diameter and a short focal length should be used to focus the light onto the detector.

Since the bandwidth of the excitation laser is often much larger than the (residual) mode spacing, many modes are excited. As shown by Hodges *et al.* (1996b), the excitation of many (transverse) modes dramatically reduces the modulation depths of the beats observed in the ring-down transients. By making the cavity mechanically unstable, the mode spacings vary, assuring that all frequencies are coupled into the cavity with an 'equal probability' (this also assures that the ratio of transverse and longitudinal modes is most of the time irrational). When the ring-down transients are averaged, the residual mode beating effects are further minimized, leading to a single-exponentially decaying transient. Note that mode beating effects in the transient are often difficult to observe owing to a 'slow' detector response or electronic filtering.

There are a few disadvantages of the continuum-mode approach. First of all, the spatial resolution of CRD spectroscopy is not optimal because of the spatial extent of the transverse modes. Spatial resolution is important in experiments where one wants to map out the spatial distributions of molecular species (see for example Zalicki *et al.* (1995a) and Zhao *et al.* (2000)). Exciting only longitudinal modes ('TEM_{00} mode matching') improves the spatial resolution and can be achieved by using mode-matching optics to couple the laser light into the cavity, or by using small-diameter mirrors (Romanini and Lehmann 1993), or by placing apertures in the cavity (Zalicki *et al.* 1995a, Hodges *et al.* 1996b).

Another disadvantage of the continuum-mode approach is the ultimate sensitivity that can be obtained (Hodges *et al.* 1996b), which is important for quantitative high-sensitivity absorption measurements. The accuracy in the determination of the decay time is limited owing to very small quasirandom variations in the residual transverse mode beating. The ultimate sensitivity is obtained if only one single longitudinal mode is excited in the cavity, giving a truly single-exponential decay (Van Zee *et al.* 1999).

Lehmann and Romanini (1996) suggested that one can perform CRD spectroscopy with a higher spectral resolution than the laser which is used to excite the cavity. In order to perform such an experiment, the mode spacing of the cavity should be larger than the spectral width of the laser, and the cavity length should be carefully controlled in order to prevent drift of the modes. Such an experiment has been reported by Van Zee *et al.* (1999) and is described in more detail in section 2.8.

It should be noted that pure TEM_{00} mode matching is not straightforward. As shown above, observing a single-exponentially decaying ring-down transient does not have to indicate that a single mode is excited in the cavity, since this can also be due to excitation of (many) transverse modes and/or slow detector response. A charge-coupled device (CCD) camera should be used in order to visualize the mode pattern (spatial structure) of the light exiting the ring-down cavity (see for example Hodges *et al.* (1996b)). This provides a way to maximize coupling into the TEM_{00} modes.

A more extensive discussion on the mode structure in a ring-down cavity, and how this affects the ring-down transient (mode beating) and the measured absorption spectrum, can be found in the work by Zalicki and Zare (1995), Martin *et al.* (1996), Lehmann and Romanini (1996), Hodges *et al.* (1996b) and Scherer *et al.* (1997b). However, it should be emphasized that, for the majority of CRD applications, problems associated with the mode structure of the ring-down cavity are largely absent.

2.4. *Laser bandwidth effects*

It is evident from equations (1) and (2) that the CRD transient is only a single-exponentially decaying curve if the bandwidth of the laser radiation that is coupled into the cavity is much smaller than the width of the absorption features. Consider for example a strong but narrow absorption which is detected with a broad bandwidth laser whose centre frequency is set at the frequency of the absorption. Light with a frequency at the centre of the absorption line will have a short decay time whereas frequencies in the wings of the laser profile will have the decay time of the empty cavity, which is much longer. The observed ring down time, which is obtained by fitting the measured (multiexponentially decaying) transient to a single-exponentially decaying function, is predominantly determined by the contributions of the wings of the laser profile. Thus, in general, an absorption is underestimated if the bandwidth of the laser is comparable with or larger than the width of the molecular absorption. It is noted that this 'bandwidth effect' is similar to that observed in conventional absorption spectroscopy when the instrumental resolution is lower than the width of the absorption features.

The bandwidth effect in CRD spectroscopy has been investigated by Zalicki and Zare (1995), Jongma *et al.* (1995) and more quantitatively by Hodges *et al.* (1996a). These studies have shown that, for cases in which the bandwidth of the laser cannot be neglected, one can still extract the correct absorption coefficient from the measured decay transients, provided that the spectral intensity distribution of the light source is known.

Zalicki and Zare (1995) have also shown that for small absorbance the measured *integrated* absorption deviates only slightly from the true integrated absorption. The condition of small absorbance can be achieved by obtaining the ring down time τ from the early part of the decay transient. This has experimentally been demonstrated by Newman *et al.* (1999) who reported the integrated absorption intensity of the $a\,^1\Delta_g(v = 0) \leftarrow X\,^3\Sigma_g^-(v = 0)$ band of molecular oxygen, measured with two spectroscopic techniques: high-resolution Fourier transform spectroscopy with a long-path absorption cell, and CRD spectroscopy. In their CRD experiment the laser bandwidth was 0.25 cm^{-1}, while the pressure- and Doppler-broadened linewidths of oxygen were only 0.098 cm^{-1}. By limiting the determination of the ring-down time to the first 0.5 μs of the decay transient (with a decay time of approximately 10 μs), the integrated absorption intensity obtained from the CRD experiment was in excellent agreement with that obtained from the Fourier transform experiment.

2.5. *Multiplex cavity ring-down spectroscopy*

Quantitative information is most easily extracted from the CRD measurements when the bandwidth of the laser can be neglected relative to the width of the absorption features (see section 2.4). If this is no longer valid, knowledge of the spectral intensity distribution of the laser is required in order to obtain the correct absorption coefficients. Therefore, one can also use a polychromatic light source and extract the spectral information after spectrally dispersing the light exiting the cavity. For this the temporal shape of the ring-down transient has to be recorded and analysed for a specific frequency (interval). A monochromator with a suitable detector or a time-resolved optical multichannel analyser can for instance be used. Another possibility is to couple the polychromatic light exiting the cavity into a Michelson interferometer. The time dependence of the ring-down transient per frequency interval

is found after Fourier transformation of the measured time dependence of the (spectrally integrated) ring-down transients recorded at well defined interferometer arm length differences.

This so-called Fourier transform cavity ring-down (FT-CRD) scheme has been described and demonstrated by Engeln and Meijer (1996). In their experiment they recorded the FT-CRD spectrum of the A band of molecular oxygen around 762 nm. The light of a broad-band pulsed dye laser with a spectral width of about 400 cm^{-1} was coupled into the CRD cell 45 cm long with a near-continuum-mode spectrum. The light exiting the cavity was coupled into a multimode fibre which was connected to a FT spectrometer (Bruker IFS 66v with the step-scan option). At every mirror position the multiexponentially decaying transients were measured with a PMT, digitized with an oscilloscope and stored on a PC. After the complete measurement, the data were rearranged so that, at each time point, interferograms were formed (i.e. signal as a function of mirror position). These interferograms were Fourier transformed to obtain the spectral intensity distribution at each time point. By again rearranging the data so that at each frequency the time points were collected, a ring-down transient at that frequency was obtained, from which τ was determined. In this way the absorption spectrum of oxygen was 'constructed'. The resolution of a FT-CRD spectrum is determined by the resolution of the FT spectrometer. In FT-CRD spectroscopy, the absorption is deduced from the temporal shape of the ring-down transient; therefore, only the spectral shape of the light source has to be known and has to remain constant during the measurement, whereas the intensity of the light source is allowed to fluctuate; one does not need to know the absolute intensity of the interferograms.

The signal-to-noise ratio and the resolution of the spectrum of oxygen recorded with the FT-CRD technique is not as good as can be obtained with a tuneable narrow-band pulsed dye laser (with the same data acquisition time and under the same experimental conditions (Engeln and Meijer 1996)). Because of the narrow width of the oxygen transitions, one has to record interferograms at many positions of the moving mirror of the FT spectrometer. Together with the mathematical conversion of the data, this is rather time consuming. Therefore, the FT-CRD technique is especially suitable when spectrally broad survey scans have to be made or when broad spectral features have to be recorded. The technique can also be used to enhance the resolution of the pulsed laser. This has been shown by Engeln *et al.* (1997b), who have recorded the FT-CRD absorption spectrum of ethylene around 10.5 μm using an intrinsically broad-band laser pulse from a free-electron laser.

Instead of a FT spectrometer one can also use a monochromator for dispersing the light exiting the cavity. One can scan the monochromator and measure the ring-down transient at each wavelength (Crosson *et al.* 1999), or one can use a time-resolved optical multichannel analyser for recording the transients at many wavelengths simultaneously. This latter approach has been demonstrated by Scherer (1998). In his ring-down spectral photography (RSP) technique the time and frequency response of the cavity are recorded simultaneously along orthogonal axes of a two-dimensional array detector. The light exiting the cavity is dispersed in time with a high-speed rotating mirror and in wavelength with a diffraction grating and imaged on a CCD camera. In the initial proof-of-principle study, Scherer (1998) measured the fifth overtone spectrum of propane in the 635 nm region with a narrow-band pulsed dye laser which is tuned over the absorption band. Although not yet demonstrated, the use of a broad-band light source results in a continuous image of wavelength versus time, a 'spectral photograph', which can be converted to yield an absorption spectrum by

fitting the decay constants of the time traces. RSP offers possibilities for real-time monitoring of molecular species.

2.6. *Polarized light in cavity ring-down spectroscopy*

Most CRD experiments are performed with linearly polarized light, although the polarization of the light is not explicitly used. Nevertheless CRD experiments can be designed which make use of the polarization state of the light. Already in 1990, Le Grand and Le Floch had shown that, by placing polarization-selective elements in front of and behind the ring-down cavity, the linear or circular dichroism in either optical or atomic systems can be measured, but it was only in 1997 that polarized light was used in CRD spectroscopy of molecules.

Two examples will be presented which show the application of polarized light in molecular spectroscopy. In the first, the rotationally resolved spectra of the $b\,^1\Sigma_g^+(v = 0) \leftarrow X\,^3\Sigma_g^-(v = 0)$ band of molecular oxygen are recorded by CRD spectroscopy in magnetic fields up to 20 T (Berden *et al*. 1998). The absorption spectra are measured with linearly and circularly polarized light, leading to different ΔM selection rules in the molecular transition, thereby aiding in the assignment of the spectra. In the second example it is demonstrated that use can be made of the polarization state of the light in the cavity to improve further on the sensitivity and species selectivity of the CRD method. This polarization-dependent cavity ring-down (PD-CRD) technique, which is the CRD analogue of MRS, extends the applicability of the CRD method to the accurate measurement of magneto-optical phenomena, such as polarization rotation (Engeln *et al*. 1997a).

2.6.1. *Spectroscopy with polarized light*

The rotationally resolved spectra of the $b\,^1\Sigma_g^+(v = 0) \leftarrow X\,^3\Sigma_g^-(v = 0)$ band of molecular oxygen have been recorded in magnetic fields up to 20 T in order to validate the theoretical model that is used to describe the interaction between the oxygen molecules and the magnetic field (Berden *et al*. 1998). With this model it is possible to calculate the spin contribution to the molar magnetic susceptibility of oxygen as a function of the magnetic field strength and the temperature. Furthermore, it can be shown that molecular oxygen is aligned in high magnetic fields. This is a nice example of a molecular system in which the alignment is caused by the spin–spin interaction via a coupling of the spin angular momentum to the magnetic field direction. Additionally this study demonstrates that sensitive direct absorption spectroscopy can be applied in short cavities in environments that are difficult to access, such as inside a high-field magnet.

Since the magnetic field was homogeneous over a few centimetres, a very short ring-down cavity has been used in order to prevent the spectra from becoming too complex. The length of the cavity was chosen such that the broadening of the rotational lines due to the inhomogeneity of the magnetic field was comparable with the combination of Doppler and pressure broadening. The ring-down cavity was formed by two plano-concave mirrors with a diameter of 25 mm and a radius of curvature of -1 m, placed 3 cm apart. The mirrors were mounted on a short tube, in a fixed position relative to each other. This short cavity was placed inside a cell 84 cm long, which was inserted in a Bitter magnet with a bore of 3·1 cm. The axis of the cavity was parallel to the magnetic field lines (Faraday configuration). The cavity was positioned in the centre of the magnet in a region where the field was rather homogeneous; the field at the position of the mirrors dropped to 98·5% of the

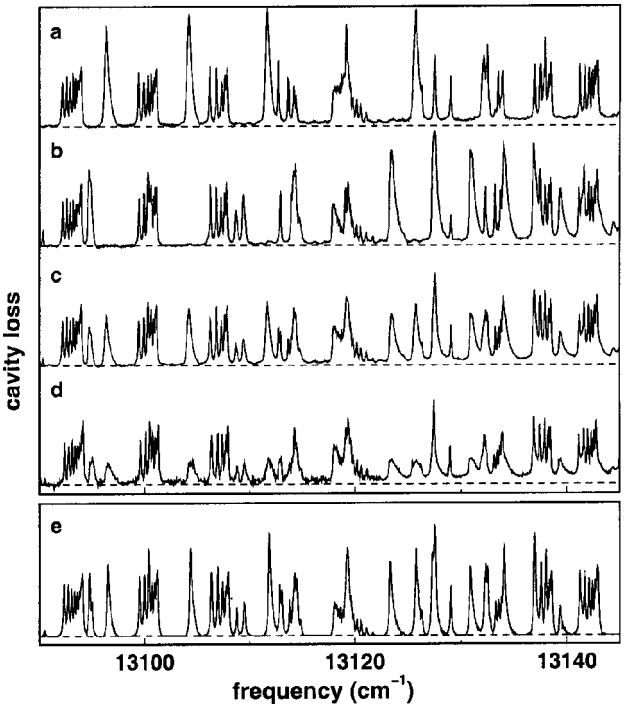

Figure 4. CRD spectra of molecular oxygen at 20 T: (*a*) the measured spectrum with σ^+-polarized light; (*b*) the measured spectrum with σ^--polarized light; (*c*) the sum of the spectra shown in (*a*) and (*b*) divided by 2; (*d*) the measured spectrum with linearly polarized light; (*e*) the simulation of the spectrum with linearly polarized light. The vertical scales are the same for each spectrum. When CRD spectroscopy in a magnetic field is performed with linearly polarized light, absorptions induced exclusively by σ^+ or σ^- light are underestimated. (Figure reproduced from Berden *et al.* (1998) with permission. Copyright the American Physical Society).

maximum field at the centre of the cavity. The cell was filled with pure molecular oxygen (100–500 mbar) and holes in the small ring-down cavity tube allowed the oxygen to enter the cavity as well.

Pulsed-laser radiation at a wavelength of 762 nm was obtained from a pulsed dye laser (10 Hz repetition rate and 5 ns duration pulses), delivering pulses with several millijoules of energy in a spectral profile with a bandwidth of approximately 0.07 cm^{-1}. Prior to entering the cell with the ring-down cavity, the incoming laser beam passed through a Glan–Thompson polarizer, creating linearly polarized light. Optionally, by placing a $\lambda/4$ plate between the Glan–Thompson polarizer and the entrance window of the cell, circularly polarized light was created. Since the PMT could not be placed in the neighbourhood of the Bitter magnet, the light exiting the cavity was coupled into a fibre 13 m long which was connected to the PMT. The time constant τ that described the decay of the light in the empty cavity in our set-up was around 350 ns, corresponding to an effective absorption path length of 105 m (for one τ) and an effective reflection coefficient $R \approx 0.9997$.

Figures 4 (*a*), (*b*) and (*d*) show three CRD absorption spectra of oxygen measured in a magnetic field of 20 T using different polarization states of the light, namely right-hand circularly polarized (σ^+), left-hand circularly polarized (σ^-) and linearly polarized respectively. Comparison of the spectra in figures 4 (*a*) and (*b*) shows that the

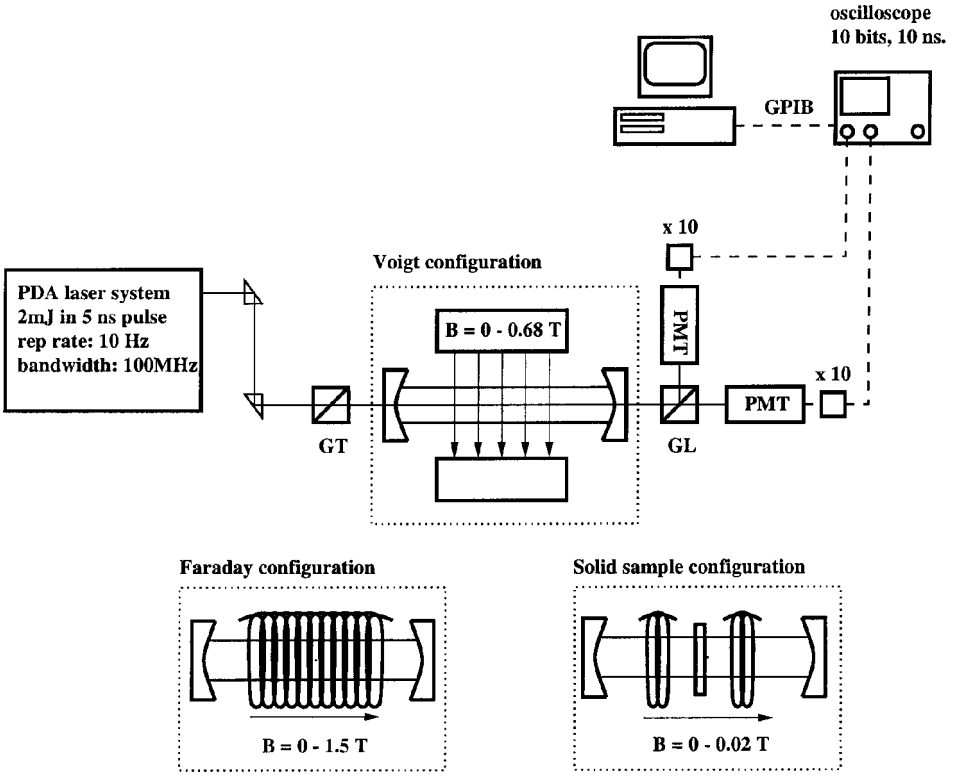

Figure 5. Schematic view of the experimental set-up for PD-CRD spectroscopy: PDA, pulsed dye amplified; GT, Glan–Thompson polarizer; GL, Glan laser polarizer; PMT, photomultiplier tube; GPIB, general-purpose interface bus. Pulsed-laser radiation is coupled into a ring-down cavity. Prior to entering the cavity, the light passes through a Glan–Thompson polarizer. The light exiting the cavity is split by a Glan laser polarizer into two mutually orthogonally polarized components that are recorded independently. In the Faraday configuration for the solid sample, two Helmholtz coils are used to create the magnetic field. (Figure reproduced from Engeln *et al.* (1997a) with permission. Copyright the American Institute of Physics).

polarization state of the light is not (or hardly) affected by the multiple reflections on the mirrors of the cavity. In addition, the sum of the σ^+ and σ^- spectra (divided by 2) is shown in figure 4 (*c*). This sum spectrum should be identical with the spectrum measured with linearly polarized light but, although all features can be found in both spectra, it is seen that the intensity of strong features which arise *solely* from $\Delta M = +1$ *or* $\Delta M = -1$ transitions are underestimated in the measured spectrum. This is an experimental artefact that can be understood by realizing that, at such a transition, only one of the circularly polarized components can be absorbed, while the other is not affected at all. Since the transient measured at the exit of the cavity is fitted to a single-exponentially decaying curve, the absorption is underestimated. A comparable effect occurs when the bandwidth of the light source is larger than the linewidth of the absorption (see section 2.4). However, note that the 'polarization' effect is also present when the laser line width is infinitely small.

2.6.2. *Polarization-dependent cavity ring-down spectroscopy*

By placing a polarization-selective optical element in front of the detector (e.g. a polarizer), it is possible to measure the rotation of the plane of polarization of the incoming linearly polarized beam upon passage through the ring-down cavity. If (part of) the cavity is placed inside a magnetic field, the plane of polarization can rotate owing to dispersion (magnetic birefringence) or polarization-dependent absorption (magnetic dichroism). The experimental set-up for PD-CRD spectroscopy which has been used to measure these magneto-optical effects on molecular oxygen (Engeln *et al.* 1997a) is shown in figure 5. The ring-down cavity with a length d is placed inside a magnetic field which extends over a length l. Before the light enters the cavity, it passes through a Glan–Thompson polarizer. In the Voigt configuration (cavity axis is perpendicular to the magnetic field) the polarizer is used to define the angle ϕ_B between the polarization direction of the light and the direction of the magnetic field. In the Faraday configuration (cavity axis is parallel to the magnetic field) the polarizer is used to define the degree of polarization of the light better. The light exiting the cavity is sent through a Glan laser polarizer, split into its two mutually orthogonally polarized components and measured with two identical PMTs. The axis of the analyser can be oriented at an angle ϕ_D relative to the polarization direction of the incoming beam.

The time dependences of the light intensity for both polarization directions are measured simultaneously. The decay times τ are determined in the same way as in 'conventional' CRD. In the Voigt configuration the difference between the cavity losses in the two directions is given by (Engeln *et al.* 1997a)

$$\frac{1}{c\tau_{\phi_D}(\nu)} - \frac{1}{c\tau_{\phi_D+90°}(\nu)} = \frac{l \sin(2\phi_B)}{d \sin(2\phi_D)}[\kappa_{\parallel}(\nu) - \kappa_{\perp}(\nu)], \tag{5}$$

in which $\kappa_{\parallel}(\nu)$ and $\kappa_{\perp}(\nu)$ are the absorption coefficients for absorptions induced by light that is polarized parallel and perpendicular respectively to the magnetic field. Compared with 'conventional' CRD spectroscopy there is a gain in the intensity by a factor $\sin(2\phi_B)/\sin(2\phi_D)$, and there is a sign difference between absorptions polarized parallel and perpendicular to the magnetic field. Experimentally it is found that there is a reduction in the noise in the spectrum, noise that is probably associated with variations in the mode structure. Since this noise appears in the signals of both polarization directions, it cancels out in the difference signal.

In the Faraday configuration the difference between the cavity losses is given by (Engeln *et al.* 1997a)

$$\frac{1}{c\tau_{\phi_D}(\nu)} - \frac{1}{c\tau_{\phi_D+90°}(\nu)} = \frac{2\omega l}{cd \sin(2\phi_D)}[n_+(\nu) - n_-(\nu)], \tag{6}$$

in which $n_+(\nu)$ and $n_-(\nu)$ are refractive indices for right and left circularly polarized light. In this set-up, one is therefore selectively sensitive to polarization rotation, a quantity that cannot be measured in 'conventional' CRD spectroscopy. As in CRD absorption spectroscopy, where the *rate* of absorption is measured, in PD-CRD the *rate* of optical rotation is measured, and this enables the optical rotation to be put on an absolute scale.

It is important that ϕ_D is not equal to 90°, but it should be chosen such that the ring-down transients are single-exponentially decaying functions for either polarization direction. Note that PD-CRD is only sensitive for paramagnetic species, for example oxygen. Absorptions of other species are detected in both polarization directions but

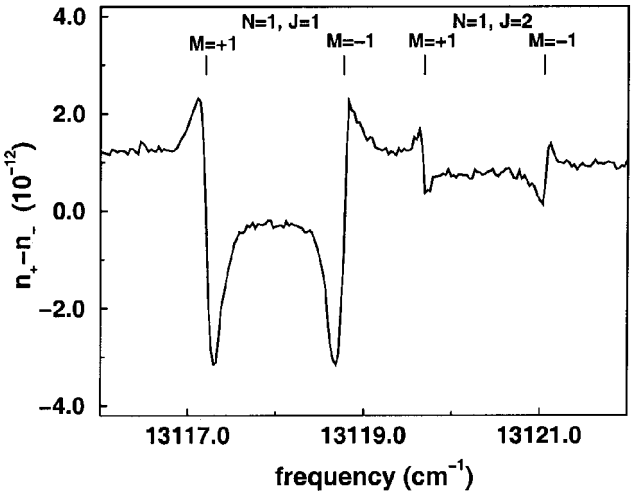

Figure 6. PD-CRD dispersion spectrum in the region of the $^{P}P(1,1)$ transition in the A band of molecular oxygen at 200 mbar. Measurements are performed in a 3 cm cavity which is placed in a magnetic field of 1·5 T. The magnetic field, which is parallel to the cavity axis, splits the transition into two components. The two small dispersion curves belong to the $^{P}O(1,2)$ transition, which becomes allowed through magnetic-field-induced mixing with the $^{P}P(1,1)$ transition. The dispersion curves are labelled with the quantum numbers of the $X\,^{3}\Sigma_g^-$ state. (Figure reproduced from Berden *et al.* (1998) with permission. Copyright by the American Physical Society).

cancel out in the difference spectrum. The PD-CRD technique has been demonstrated on the $b\,^{1}\Sigma_g^+(v'=2) \leftarrow X\,^{3}\Sigma_g^-(v''=0)$ transition of molecular oxygen around 628 nm, by measuring either the polarization-dependent absorption or the magneto-optical rotation of oxygen in the appropriate set-up (Engeln *et al.* 1997a). Figure 6 shows part of the magneto-optical rotation spectrum of the $b\,^{1}\Sigma_g^+(v'=0) \leftarrow X\,^{3}\Sigma_g^-(v''=0)$ transition of molecular oxygen around 762 nm.

2.7. *Cavity ring-down spectroscopy on surfaces, thin films, liquids and solids*

Although most CRD experiments have been performed on gas-phase species, there are a few studies which report a successful extension of the CRD technique for the application on solids. Schemes have been developed for measuring dichroism in an optical element (quarter-wave plate) (Le Grand and Le Floch 1990), phase retardances of highly reflective mirrors (Jacob *et al.* 1994), magnetic rotation in optically transparent solids (Engeln *et al.* 1997a), absorption in thin solid films (Engeln *et al.* 1999b) and absorption at surfaces (Pipino *et al.* 1997b).

Le Grand and Le Floch (1990) measured the residual reflectivity of an antireflection-coated quarter-wave plate by placing this plate in a cavity that was formed by a plane input mirror and a concave ($r = -300$ cm) mirror. The reflectivity of the mirror coatings was greater than 0·999, and their spacing was made large (270 cm) in order to have decay times as long as possible. In front of and behind the cavity they placed linear polarizers. Inserting the quarter-wave plate in the cavity reduced the decay time to about 500 ns. The quarter-wave plate, which acts itself as a Fabry–Pérot etalon, was tilted such that one of the (incident) polarized light directions had maximum transmission, while the orthogonal polarization component had a minimum transmission. The decay time of the 'resonant' polarized light was 830 ns,

while the decay time of the 'antiresonant' polarized light was 360 ns. Since the difference between the cavity losses in both directions is proportional to the reflectivity of the quarter-wave plate, they determined the residual reflectivity to be 0.35%.

If an optically transparent sample is placed inside the cavity in such a way that all resulting cavities are optically stable, reflections from the surface of the sample will remain in the ring-down cavity and thus will not be noticed as overall losses from the cavity. Of course, compared with the empty cavity there will be additional losses due to, for example, absorption in the solid and reflections of the sample which can no longer be captured in the ring-down cavity.

We have used this approach to measure the polarization rotation as a result of the Faraday effect in a optically flat BK7 window 2 mm thick using the PD-CRD scheme (see figure 5) (Engeln *et al.* 1997a). In order to avoid any interferences with ambient air (especially oxygen), the first polarizer, the ring-down cavity with the sample, and the coils that produced the magnetic field were placed inside vacuum. At a wavelength of 618.79 nm, the ring-down time of the cavity with sample and no magnetic field was about 700 ns. Thus light passed through the sample about 1100 times in one decay time. By measuring the difference signal given by equation (6) as a function of the magnetic field strength (0–6 mT) we were able to determine the Verdet constant of this BK7 window (at a magnetic field strength of 2 mT the polarization rotation was about 2×10^{-5} rad per passage).

The same approach has been used to record the absorption spectrum of a C_{60} film 20–30 nm thick deposited on a ZnSe substrate 3 mm thick in the 8.5 μm region (Engeln *et al.* 1999b). The ring-down cavity is formed by two identical plano-concave mirrors (radius r of curvature of -1 m) placed at a distance d of 36 cm apart. Tuneable pulsed radiation was obtained from an IR free-electron laser. The measured decay time of the empty cavity at 8.5 μm was 5.6 μs, implying a reflectivity of 0.9998. Inserting the optically flat ZnSe window (without the C_{60} film) reduced the decay time to 2.2 μs. Absorption of the thin film caused an additional loss determined by $\kappa l/d$, in which κ is the absorption coefficient and l the thickness of the film. The absorption spectrum of the C_{60} film 20–30 nm thick recorded between 8.1 and 8.9 μm showed a resonance at 8.45 μm which is one of the four IR-active fundamental modes of C_{60}. The peak absorption is 0.24 μm^{-1} and the full width at half-maximum (FWHM) was about 0.1 μm.

The aforementioned approach requires that the sample is optically transparent. Pipino *et al.* (1997b) have placed a fused-silica Pellin–Broca prism with ultra smooth facets under Brewster's angles in the ring-down cavity. Surface processes at the plane of total internal reflection (TIR) of the prism have been probed by CRD through absorption of the associated evanescent wave by a submonolayer of adsorbed iodine. This is a successful demonstration of the combination of attenuated total reflectance spectroscopy (which uses evanescent waves for probing optical absorptions) with CRD spectroscopy. Pipino *et al.* determined a minimum detectable coverage of 0.04 monolayer of iodine at 625 nm. The same group has theoretically outlined that, by using a TIR minicavity, absorption spectra of either thin solid films or species in solution are measurable via evanescent wave absorption spectroscopy (Pipino *et al.* 1997a). Since this set-up does not require the ultrahigh-reflectivity dielectric mirrors generally used in CRD, it can be used in a much broader wavelength range. This is especially advantageous for spectroscopy on liquids and solids which often have broad spectral features. Such a TIR minicavity requires optical materials with low bulk losses and ultrasmooth polished surfaces. Recently, Pipino (1999) reported the first successful

experiment. He used a 7.5 mm × 7.5 mm × 5.0 mm square fused silica cavity, with facets which were polished to 0.05 nm rms surface roughness. One facet was convex (2.23 cm radius of curvature) in order to form a stable optical resonator. Light enters and exits the ring cavity by photon tunnelling through coupling prisms. The losses of this cavity were dominated by bulk losses; the ring-down time ranged from 200 ns at 450 nm up to 1.3 μs at 580 nm. In the actual experiment, one facet had been exposed to iodine vapour, and the ring-down times of s- and p-polarized light were measured at a wavelength of 580 nm. Both polarizations showed a decrease in decay time as a result of optical absorption of iodine in the evanescent field. The decrease for the s-polarized light, however, was larger, suggesting that the iodine molecules are preferentially oriented with their molecular axis parallel to the surface of the cavity (since in this transition the transition dipole moment of iodine is along the molecular axis). For applications that do not require a broad bandwidth, Pipino (2000) designed a different monolithic cavity consisting of two ultrahigh-reflection-coated planar surfaces, thereby facilitating the in-coupling and out-coupling of the light, and one convex surface acting as a TIR mirror.

2.8. *Quantitativity and sensitivity of cavity ring-down spectroscopy*

The absorption coefficient is obtained from a CRD spectrum after subtracting the cavity loss measured without the absorber. In practice, however, one determines the cavity loss without absorber from the baseline in the spectrum. Thus, rewriting equation (3),

$$\kappa(\nu)\frac{l}{d} = \frac{1}{c\tau} - \frac{1}{c\tau_0} = \frac{\tau_0 - \tau}{c\tau_0\,\tau}, \tag{7}$$

in which τ_0 is the decay time measured without absorber (Van Zee *et al.* 1999). This equation shows that measuring the absorption coefficient simply involves the determination of two time constants. Furthermore, it shows that, for a simple static cell experiment where $l = d$, the absorption coefficient does not depend on the actual length of the cell. Therefore, the quantitativity of a CRD experiment is determined by the accuracy with which the ring-down times can be determined.

The minimum detectable absorption in CRD spectroscopy depends on the reflectivity R of the mirrors and on the accuracy in the determination of τ (Zalicki and Zare 1995):

$$[\kappa(\nu)\,l]_{\min} = (1 - R)\left(\frac{\Delta\tau}{\tau}\right)_{\min}. \tag{8}$$

It should be emphasized that R in this equation is in fact R_{eff} which is smaller than (or equal to) the reflectivity of the mirrors (see section 2.1). Equation (8) shows an attractive feature of CRD spectroscopy; in order to achieve high sensitivity in the absorption measurement, only a rather low accuracy in the time measurement is needed. For example, an accuracy for the determination of τ of only 1% combined with a cavity 10 cm long consisting of mirrors with a reflectivity of 99.999% leads to a minimum detectable absorption of 10^{-8} cm^{-1}.

The obtainable accuracy of τ is determined by many factors, for example, the laser system (bandwidth, modes and power), cavity (mirror reflectivity and modes), detector, data acquisition and data analysis. In most of the reported CRD experiments the accuracy of τ is of the order of a per cent, which is due to multimode excitation of

the ring-down cavity (see section 2.3). The sensitivity of CRD spectroscopy can thus be increased by single-mode excitation of the cavity.

This single-mode approach has been demonstrated by Van Zee *et al.* (1999). Their pulsed-laser system (an injection-seeded pulsed OPO) had a bandwidth of about 115 MHz (FWHM). In order to be able to excite only one cavity mode, the cavity length should be rather short. The combination of a cavity 10.5 cm long and a mirror curvature of 20 cm gave longitudinal and transverse mode spacings of 1.5 GHz and 500 MHz respectively. Mode-matching optics maximized the coupling into the lowest-order transverse mode (TEM_{00}). In this geometry, a single longitudinal mode could be excited, which led to a single-exponentially decaying ring-down transient. The relative standard deviation $\Delta\tau/\tau$ of 0.03% in the ring-down time extracted from a fit to an individual ring-down curve was found to be identical with that for an ensemble of a hundred independent measurements. CRD absorption specra of the $^{P}Q(9)$ transition of the A band of molecular oxygen were obtained by simultaneously scanning the laser and the cavity length. A noise-equivalent absorption coefficient of 5×10^{-10} cm^{-1} Hz$^{-1/2}$ was demonstrated. Furthermore, Van Zee *et al.* showed that the standard deviation for repeated measurements of the line strength was less than 0.3%.

Summarizing, CRD spectroscopy offers a sensitivity of 10^{-6}–10^{-9} cm^{-1} with a rather simple experimental set-up. The sensitivity can be increased by exciting a single longitudinal mode. This single-mode approach is experimentally more involved than the 'normal' (i.e. multimode) CRD approach, which is due to the locking and simultaneously scanning of the laser and the ring-down cavity.

3. Continuous-wave cavity ring-down spectroscopy

Excitation of a single longitudinal mode of the ring-down cavity provides the best sensitivity. For pulsed CRD spectroscopy, this implies that a FT-limited pulsed laser should be used in combination with a short cavity (see section 2.8). In this case, the length of the cavity (and thus the modes) should be scanned simultaneously with the laser wavelength, in order to record a CRD absorption spectrum. An alternative is the use of CW lasers which have to be switched off in order to observe a ring-down transient. The bandwidth of these lasers is very small (typically less than a few megahertz); therefore longer cavities can be used, resulting in longer ring-down times. In the literature, CRD spectroscopy performed with a CW laser is called CW-CRD spectroscopy, but it should be realized that this technique is in fact not a CW technique at all.

Whether pulsed CRD or CW-CRD should be used depends strongly on the application. Pulsed dye lasers and OPOs can be scanned over a large wavelength region. Furthermore, their power is high enough that nonlinear conversion techniques (frequency mixing and Raman shifting) can be used to extend the wavelength region to the UV and IR. CW lasers, on the other hand, can only be scanned over small wavelength regions and are not (yet) available at all wavelength regions. The advantage of CW-CRD is the higher repetition rate and a higher spectral resolution than can be achieved with pulsed CRD spectroscopy (the latter is only true for multimode excitation of the cavity; when exiting a single mode, the resolution in both CW-CRD and pulsed CRD spectroscopy is only determined by the width of the very narrow cavity modes). An additional advantage is an increased energy build-up inside the cavity as the linewidth of the CW laser decreases. Higher intracavity energy results in higher light intensities on the detector, improving the signal-to-noise ratios on the ring-down transients and therefore improving the sensitivity. Furthermore, compact,

easy-to-use and rather inexpensive CW diode lasers that have low power consumption and do not require cooling can be used, which are for example interesting for trace gas detection applications at remote locations. A drawback, on the other hand, is that the simplicity of the experimental set-up is abandoned, even when ultrahigh sensitivity is not needed.

3.1. *Experimental schemes*

In CW-CRD spectroscopy, this additional complexity arises from the fact that the spectral overlap between the laser frequency and the frequency of one of the cavity modes is no longer obvious. This logically emanates from the narrow linewidth of the laser (megahertz) and the high finesse of the cavity (kilohertz width of the modes). A build-up of the intracavity field will only take place if the laser frequency and a cavity mode are in resonance, for which there are several ways to proceed.

For the measurement of the reflectivity of the cavity mirrors, Anderson *et al.* (1984) used the occasional coincidences of a He–Ne laser with one of the cavity modes. When the light intensity inside the cavity exceeded a predefined threshold, a triggering system switched a Pockels cell that interrupted the laser and started the data acquisition for recording the ring-down transient. In a more controlled way, the cavity length is slowly scanned with a piezoelectric transducer, which allows repeated measurements (see for example Le Grand and Le Floch (1990) and Rempe *et al.* (1992)).

This approach has also been used by Romanini *et al.* (1997a) for measuring CW-CRD absorption spectra. The cavity length was piezoelectrically modulated in order to let one of the cavity modes oscillate around the laser line. When the light intensity inside the cavity exceeded a predefined threshold, an acousto-optical modulator (AOM) turned off the laser beam, followed by a measurement of a ring-down decay. Since they used transverse mode matching, only the TEM_{00} modes could have sufficient intensity build-up to trigger the data acquisition system. A feedback circuit measured the distance of the position of the mode responsible for the ring-down transient with respect to the centre of the modulation range and provided a correction voltage to the piezoelectric transducer. In this way they were able to record ring-down transients at a range of 200 Hz while the laser was scanned in wavelength. With this CW-CRD method, Romanini *et al.* (1997a) measured a part of the C_2H_2 overtone spectrum around 570 nm, using a CW ring dye laser, with a sensitivity of 10^{-9} cm^{-1}. Using an external cavity diode laser around 775 nm, Romanini *et al.* (1997b) demonstrated a sensitivity of 2×10^{-10} cm^{-1}, and they recorded part of the rotationally and vibrationally cooled spectrum of NO_2 in a slit nozzle expansion. In the jet experiment, their tracking system had problems with sudden fluctuations of the cavity length owing to mechanical vibrations of the pumping system. Note that the tracking system is not needed if the modulation of the cavity length is slightly more than one free spectral range and if the modulation speed is not too slow (Romanini *et al.* 1997b, and He *et al.* 1998). Instead of modulating the cavity modes, one can also modulate the frequency of the laser (Romanini *et al.* 1997b, Schulz and Simpson 1998). However, this approach can only be used if the width of the absorption features is much larger than the free spectral range of the cavity. This scheme is, for example, attractive when external cavity diode lasers are used to detect absorptions at atmospheric pressure (Schulz and Simpson 1998).

The above mentioned CW-CRD scheme in which the cavity length is modulated can also be used without an optical switch. With a piezoelectric transducer, Hahn *et al.* (1999) swept a cavity mode into resonance with the laser. When the intensity on the detector exceeded a predefined value, a switching circuit was triggered which

discharged the piezoelectric transducer. In this way, the cavity length changed a quarter-wavelength in 1 μs, causing the cavity mirror to move off resonance within a few nanoseconds. The mirror was held at this off-resonance position until a complete ring-down transient was recorded. Although no AOM or Pockels cell was used, Hahn *et al.* (1999) still needed a switching circuit. He and Orr (2000) used only the rapidly swept cavity. The resonance frequency of the cavity was swept continuously through the laser frequency on a time scale that is much shorter than the ring-down time of the cavity. A time gate was used to select one resonance during each single sweep for display on the digitizing oscilloscope. The measured transient started with a rapid increase in the intensity, when the cavity mode comes into resonance with the laser frequency. Then, the mode scans out of resonance, and the ring-down decay starts. In the early part of the decay, oscillations were observed, which limited the determination of the ring-down time to the last part of the decay transient. These oscillations are caused by the beating between the laser frequency and the cavity mode frequency, which is Doppler shifted owing to the moving mirror (see Poirson *et al.* (1997), and references therein, Hahn *et al.* (1999) and He and Orr (2000)). In fact, from these oscillations, one can determine, in specific cases, the velocity of the moving mirror (An *et al.* 1995) and the finesse (and thus the losses) of the cavity (Poirson *et al.* 1997).

Paldus *et al.* (1997) did not scan the cavity modes into resonance with the diode laser line, but instead they used a quasicontinuum mode structure (see sections 2.3 and 4) to enhance the incoupling efficiency. In this way, repetition rates up to 50 kHz could be achieved. However, higher-order transverse modes were excited, limiting the accuracy in the determination of the ring-down time. Nevertheless, their initial experiments showed already a sensitivity which is comparable with most pulsed CRD studies, and a tracking system was obviously not needed.

When the CW laser is in resonance with the cavity mode, a large fraction of the light, depending on the bandwidth of the laser with respect to the width of the cavity modes, is coupled into the cavity, but also a large amount of light is coupled out of the cavity in the direction of the detector and in the direction of the laser. This strong optical feedback induces mode hops (jumps in wavelength) of the laser, thus breaking the resonance and causing irregularities in the wavelength scan. Therefore, an optical isolator is needed between the laser and the cavity. The AOM which also turns off the laser beam can be used for this purpose (Romanini *et al.* 1997a), but sometimes this modulator alone does not give enough isolation and an additional Faraday isolator is used (Paldus *et al.* 1997, Romanini *et al.* 1997b).

Active locking of a cavity mode to the frequency of the laser, which would lead to higher and more reproducible intracavity energies and therefore less variation in the ring-down times, is not straightforward since the laser has to be switched off in order to record a ring-down transient.

Paldus *et al.* (1998) used a sophisticated scheme to record ring-down transients while the cavity is locked to the laser. The key concept is that the laser beam is split into two beams with orthogonal polarizations ; one beam is used to lock the ring-down cavity continuously to the laser, while the other beam is used to measure ring-down transients. Their ring-down cavity consisted of three mirrors. In this way, the optical feedback from the ring-down cavity was absent. Furthermore, the orthogonally polarized light beams will now see different mirror reflectivities as they are incident under non-normal angles. Consequently, the cavity will have different finesses for both beams. The low-finesse resonator was used for the locking of the cavity to the laser mode, while the high-finesse resonator was used to perform CW-CRD spectroscopy.

Both polarized beams are simultaneously resonant in the cavity, and the cavity can, therefore, be continuously locked to the laser even when the beam used for CRD is switched on and off by an AOM. The decay transient was detected and analysed in the usual way, but an improvement of the sensitivity can be obtained by using optical heterodyne detection (Levenson *et al.* 1998, 2000). Despite the greater complexity involved in this active locking approach, it is a promising way to achieve higher sensitivities (section 3.2) (Spence *et al.* 2000).

Recently, Ye and Hall (2000) presented a scheme that offers a quick comparison of on- and off-resonance information. Two cavity modes, one probing the empty cavity losses and the other probing the total cavity losses (including molecular absorption), were excited simultaneously. The intensities of the modes were temporally out of phase, with one mode decaying and the other rising. This was achieved with two AOMs that also provided the necessary frequency offset. Heterodyne detection between the two modes yielded the molecular absorption.

3.2. *Sensitivity*

Exciting a single longitudinal mode of the ring-down cavity provides the best sensitivity, just as in pulsed CRD spectroscopy (see section 2.8). By locking the cavity to the laser line, the energy build-up in the cavity is high, which results in a high intensity on the detector that records the ring-down transient, thus improving the signal-to-noise ratio. With a locked cavity consisting of three mirrors with a reflectivity $R = 0.9993$, Paldus *et al.* (1998) achieved a sensitivity of 5×10^{-9} cm^{-1}. Although the repetition rate could in principle be more than 10 kHz, the actual repetition rate was only a few hundred hertz, limited by the acquisition speed of the digitizing electronics. Furthermore, the sensitivity of their spectrometer was limited by electronic noise imposed by the detection electronics (e.g. the digitizer).

Recently, this set-up has been spectacularly improved by using an analogue detection scheme (Spence *et al.* 2000). With this improved CRD spectrometer, they achieved a sensitivity of 8.8×10^{-12} cm^{-1} Hz$^{-1/2}$ for the detection of carbon dioxide at around 1064 nm. The cavity round-trip path was 42 cm, and the ring-down time of the empty cavity was 2.8 μs. The switching speed of the AOM, used for turning the laser beam on and off, was 80 kHz. Note that mirrors of modest reflectivity were used in order to obtain not too low intensities on the detector.

Van Zee *et al.* (1999) compared, very generally, the sensitivities which can be obtained with single-mode pulsed and CW-CRD spectroscopy. Their conclusion is that, in principle, the highest sensitivity can be obtained when a CW laser with a very narrow bandwidth is used. This is mainly due to the more efficient coupling of light into the cavity. Obviously, a real comparison between pulsed and CW-CRD spectroscopy is very difficult since detailed knowledge is needed of all components of the spectrometer.

3.3. *Applications*

CW-CRD spectroscopy is suitable for ultrahigh-resolution spectroscopy of molecules and clusters in a supersonic expansion. In general, jet spectra are much simpler to interpret than spectra recorded in a cell, because of the reduced Doppler width of the rovibrational transitions and the reduced number of spectral lines as a result of rotational and vibrational cooling. For example, Hippler and Quack (1999) recorded the jet-cooled spectrum of the $\nu_2+2\nu_3$ combination band of methane, and Biennier *et al.* (2000) recorded the rotationally resolved spectrum of an electronic transition of the O_2 dimer.

An additional advantage of CW-CRD spectroscopy is the high intracavity power which can be achieved, which offers the possibility of studying nonlinear effects (Romanini *et al*. 1999b, Bucher *et al*. 2000). Romanini *et al*. (1999b) recorded the absorption spectrum of NO_2 in a jet, using a 2 W single-mode titanium-doped sapphire laser. The power in their ring-down cavity was about 20 W, which allowed them to observe saturation effects such as decreased absorption and Lamb dips. It should be noted, however, that such nonlinear effects have also been observed with pulsed CRD spectroscopy (Lehr and Hering 1997a, Labazan *et al*. 2000).

Furthermore, CW-CRD spectroscopy can also be used for trace gas detection. For example, Campargue *et al*. (1998) demonstrated the sensitive detection of SiH_2 in a argon–silane discharge. In this context, the development of compact and low-cost diode lasers is important. Since only one (or a few) rovibrational transitions of a trace gas molecule need to be monitored, the limited spectral region in which a single diode laser operates is not a disadvantage. For example, with a multiplexed diode laser system consisting of two diode lasers operating at 1391 and 1402 nm, Totschnig *et al*. (2000) could measure, simultaneously, methanol and isopropanol in a cell with a sensitivity of 2.4×10^{-9} cm^{-1} for a 4.3 s averaging time.

4. Cavity-enhanced absorption spectroscopy

CRD spectroscopy with CW lasers can also be performed without temporal analysis of the ring-down transient. In PS-CRD, the absorption coefficient is extracted from a measurement of the wavelength-dependent phase shift that an intensity-modulated CW light beam experiences upon passing through a high-finesse optical cavity. This technique has been developed by Herbelin *et al*. (1980) for measuring mirror reflectances near unity. Engeln *et al*. (1996) have used this technique to record the absorption spectrum of the γ band of $^{18}O_2$.

In this experiment, the output of the CW laser was passed through an electro-optical modulator that sinusoidally modulated the light intensity. The intensity-modulated light was coupled into the optical cavity. No mode-matching optics were used, and the separation of the mirrors was chosen such that a very dense (near-continuum) mode spectrum was obtained (see section 2.3). In this way, the incoupling efficiency of the light was maximized. The inner diameter of the cavity 45 cm long was 8 mm, reducing the total volume of the cell to only 25 cm^3, providing a way to save on the rather expensive isotopic oxygen. The intensity of the light that leaked out of the cavity was detected with a PMT placed closely behind the optical cavity in order to ensure that all cavity modes were detected with an equal probability. The phase shift Φ of this signal is directly related to the cavity ring-down time τ via $\tan \Phi = \Omega\tau$, where Ω is the angular frequency of the modulation. This phase shift was determined with a fast lock-in amplifier.

The independence of intensity fluctuations allows the PS-CRD absorption method to be performed in optical cavities without any length stabilization. The sensitivity of this technique is comparable with that of multimode pulsed and CW-CRD techniques. Since no fit of the ring down transient is required, PS-CRD can easily be performed with analogue detection electronics. In PS-CRD spectroscopy the decay time of the light in the cavity is obtained via a measurement of the phase shift. Instead of an optical switch, which is needed in CW-CRD spectroscopy, one now needs an electro-optical modulator.

In CEA spectroscopy, no switch or modulator is used. Laser light is coupled into the cavity via accidental coincidences of the light with the cavity eigenmodes, and the

time-integrated intensity of the light leaking out of the cavity is measured. In our preliminary experiments (Engeln *et al.* 1997a), this CEA scheme was used to record the $^{P}P_1(1)$ transition of the oxygen γ band with a single-mode ring dye laser. A detailed description of the CEA technique, together with a description of relevant experimental details, has been given by Engeln *et al.* (1998). In short, the key concept is that the frequency of the laser should be in resonance with each cavity mode equally long. This can easily be done by scanning the frequency of the laser so fast that the interaction time is determined by the scanning speed of the laser, and not by the instability of the cavity. Alternatively, the laser can be scanned slowly while the cavity mode structure is scanned by moving one of the cavity mirrors.

Although we have called this experimental scheme CEA spectroscopy, in order to distinguish it from CRD spectroscopy, it is not the same as cavity transmission spectroscopy (which is also called CEA spectroscopy). In cavity transmission spectroscopy, the laser frequency is locked to the frequency of a cavity mode, and the transmission through the cavity is recorded as a function of the frequency (see for example Nakagawa *et al.* (1994), Ye *et al.* (1998) and Inbar and Arie (1999)). The high-finesse cavity is used to enhance the detection of absorptions, since its transmission is sensitive to small variations in the absorption inside the cavity. The essential difference from CRD spectroscopy is that the resonance between the laser and cavity mode is never broken. By combining cavity transmission spectroscopy with modulation techniques, Ye *et al.* (1998) reported a sensitivity of 1×10^{-14} cm^{-1} using a CW neodymium-doped yttrium aluminium garnet laser at 1.064 μm and a cavity with a finesse of 100 000. This spectacular sensitivity is superior to that achieved with CRD spectroscopy. However, the technical requirements are very high. On the other hand, the 'crude' CEA approach described in this section is very simple and technically less demanding.

4.1. *Experimental set-up and measurement procedure*

Similar to CW-CRD spectroscopy, light from a narrow band CW laser is coupled into an optical cavity formed by two highly reflective mirrors. Since the cavity acts as a frequency-selective filter, only those laser frequencies will enter the cavity that are in resonance with the cavity eigenfrequencies. In CW-CRD spectroscopy, the cavity geometry is chosen mostly in such a way that the longitudinal modes and the transverse modes are at isolated frequencies. Furthermore, mode-matching optics are used to excite mainly the longitudinal cavity modes. In CEA spectroscopy the cavity mode spectrum is chosen to be a quasicontinuum (see section 2.3).

The frequency of the laser and/or the frequencies of the cavity modes are scanned rapidly (*vide infra*) while the time-integrated intensity of the light exiting the cavity is measured with a detector placed behind the cavity end mirror. This intensity is proportional to, firstly, the finite 'resonance' time of (a fraction of) the spectral profile of the laser with the cavity mode and, secondly, the maximum intensity that can be reached inside the cavity. The resonance time is mainly determined by the scanning rate of the laser (and/or the scanning rate of the cavity mirror). This rate should be chosen so that the resonance time is equally long for each cavity mode, assuring that the frequency jitter of the cavity eigenfrequencies due to mechanical instabilities will be of hardly any influence on the resonance time. Furthermore, the interaction time must be sufficiently long in order to allow the light intensity inside the cavity to converge to its limiting value. The maximum intensity that can be reached inside the cavity is proportional to the spectral overlap of the laser profile with the profile of the

cavity mode. As the spectral profile of the cavity mode is given by the Airy function with a width proportional to the cavity losses, that is proportional to $1/\tau$, and with an intensity proportional to τ^2, the maximum intensity in the cavity is directly proportional to the ring down time τ. The results of more detailed calculations using Fabry–Pérot theory (see for example, Zalicki and Zare (1995)) and taking into account the cavity build-up and decay can be found in the paper by Engeln *et al*. (1998). In this paper it is shown that time-integrated intensity of the light leaking out of the cavity is linearly proportional to the cavity decay time τ. Thus, by plotting the inverse of the detected signal versus frequency, an absorption spectrum is obtained.

Depending on the scanning capabilities of the laser, a CEA spectrum can be obtained in various ways. When using a laser that can be scanned over a wavelength interval with a high repetition rate, as is the case with an external cavity diode laser (ECDL), the laser is scanned rapidly in time (e.g. 1 cm^{-1} at a rate of 30 Hz). The CEA signal is recorded as a function of time, which is proportional to the wavelength of the laser. As the optical cavity is mechanically unstable, the cavity length will jitter in time and, as a result, each single scan will have contributions from slightly different frequencies. Therefore, summation over several scans (typically more than 100) provides a method to sample each wavelength with an equal probability. When using a laser that can only be scanned slowly or that can only be stepped in wavelength, the cavity modes are scanned rapidly using a piezoelectric transducer mounted on one of the cavity mirrors while the signal is averaged over some time. Again, this approach allows all laser wavelengths to be coupled into the cavity. The rate at which light will be coupled into the cavity strongly depends on the mode structure of the cavity, in combination with the scanning rate of the laser or cavity and the frequency jitter of the cavity eigenfrequencies.

The limiting factor for the sensitivity of this CEA approach results from the residual mode structure which is visible on the baseline of the absorption spectrum. In order to wash out this residual mode structure fully, an additional, preferably random cavity mode jittering is required. The easiest way is to construct a mechanically unstable cavity and to make use of the vibrations, for example those generated by a rotary pump (section 4.2) (Berden *et al*. 1999). Another way is to scan both the laser wavelength and the cavity mode eigenfrequencies (section 4.3) (Peeters *et al*. 2000). When the laser wavelength is stepped or scanned slowly, and the cavity eigenfrequencies are rapidly scanned, the signal-to-noise ratio can be improved by rapidly modulating the laser wavelength (O'Keefe *et al*. 1999).

In CEA spectroscopy, the total time-integrated signal is inversely proportional to the ring-down time τ. The absorption coefficient is then given by, using equation (3),

$$\kappa(\nu) = \left(\frac{S_0(\nu)}{S(\nu)} - 1\right)\frac{1-R}{l}, \tag{9}$$

where $S(\nu)$ is the recorded time-integrated intensity with absorbing species, and $S_0(\nu)$ is the CEA signal without absorbing species (i.e. the baseline). This equation shows that an absorption spectrum is obtained by dividing the baseline by the CEA signal. Furthermore, this equation shows that the absorption coefficient is expressed in units of $(1-R)/l$. Therefore, the intensity axis in a CEA absorption spectrum of a sample, whose number density or absorption cross-section is not known, can only be obtained on an absolute scale when the mirror reflectivity is known. The mirror reflectivity can be determined in a CRD experiment, or can be calibrated by measuring the absorption

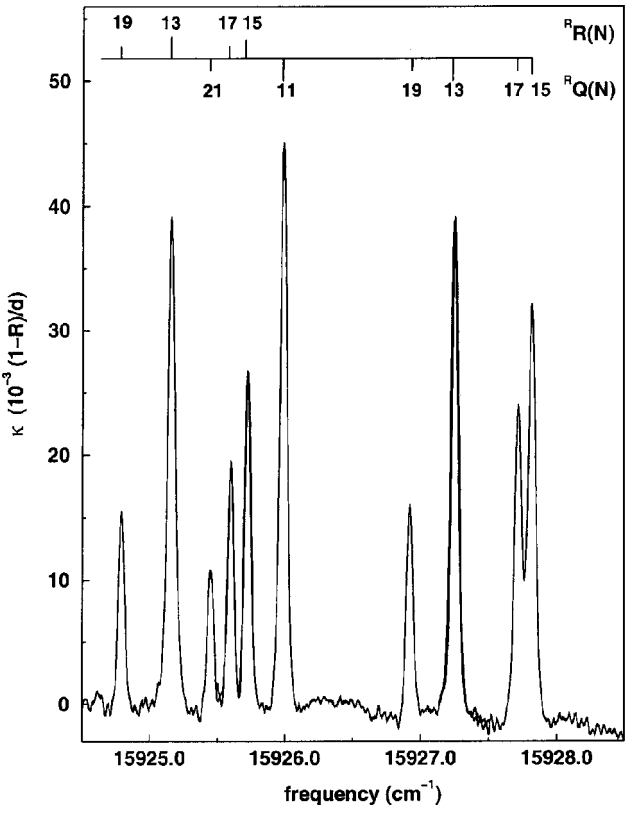

Figure 7. CEA spectrum as recorded with molecular oxygen at 200 mbar in a cell 12 cm long at room temperature, displaying the band heads in the ^{R}R and ^{R}Q branches of the γ band around 628 nm. (Figure reproduced from Engeln *et al.* (1998) with permission. Copyright the American Institute of Physics).

of molecules with a known absorption cross-section and number density. So, contrary to (CW-)CRD, CEA is not a self-calibrating absorption technique. However, it should be emphasized that the CEA spectra are of comparable quality with those obtained via (multimode) pulsed CRD or CW-CRD spectroscopy.

4.2. *Applications of cavity-enhanced absorption spectroscopy*

Since the technique has only recently been developed, only a few experiments have been performed with CEA spectroscopy which, however, give a good impression of the versatile experimental capabilities of this technique.

In figure 7 a part of the absorption spectrum of the $b\,^1\Sigma_g^+(v = 2) \leftarrow X\,^3\Sigma_g^-(v = 0)$ band of oxygen (γ band), showing the band heads of the ^{R}R and ^{R}Q branches, is shown as recorded with a CW ring dye laser in a cell 12 cm long filled with molecular oxygen at 200 mbar and room temperature. The spectrum is a compilation of three partly overlapping measurements, each covering about 1.5 cm^{-1} averaged over 100 scans. With a scanning rate of the laser of around 5 Hz, this implies an effective recording time of 1 min. The relative line intensities match calculated absorption spectra very well, thereby demonstrating the viability of the data extraction procedure. As mentioned above, the absorption is expressed in units that depend on the reflectivity of the mirrors. For these transitions of oxygen the cross-sections are

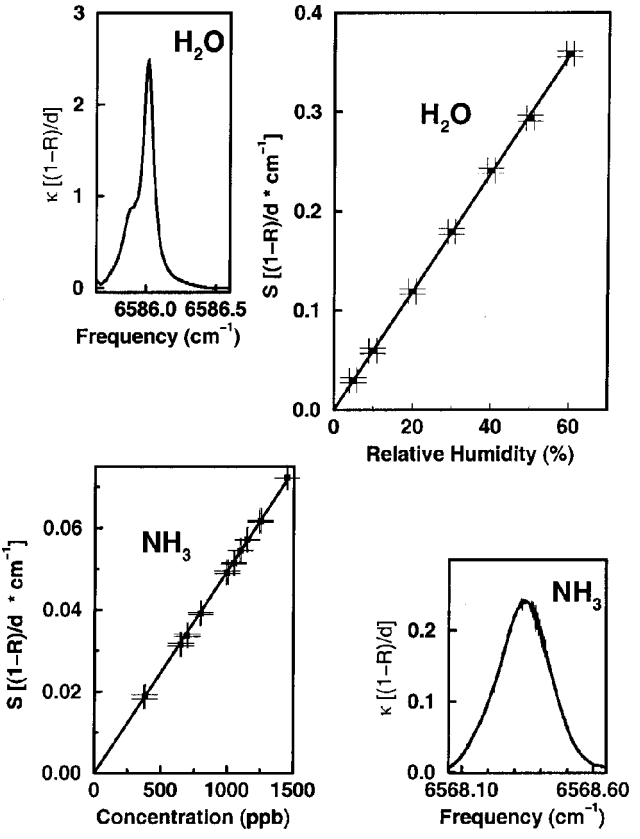

Figure 8. Linearity plot of the CEA detector. For different ammonia and water concentrations the CEA spectrum is measured. The integrated absorption S, which is equal to the area under the CEA spectrum, is plotted versus the ammonia concentration and water concentration, measured with a chemiluminescence monitor and a relative humidity sensor respectively. (Figure reproduced from Peeters *et al.* (2000) with permission. Copyright Springer Verlag).

known, providing a way to determine the reflection coefficient $R = 0.9998$, which is in good agreement with independent CRD measurements.

It is always possible to deduce absolute absorption coefficients from the CEA spectra, when the species whose absorption cross-section or number density is not known is measured simultaneously with a species with a known absorption coefficient. This has been demonstrated by recording the CEA spectrum of water at 1.0 mbar with a trace amount of ammonia using an ECDL around 1.5 μm (Engeln *et al.* 1998). With an ECDL operating at 1.3 μm, O'Keefe *et al.* (1999) have measured absorption spectra of water vapour and carbon dioxide (note that they name this technique integrated-cavity output spectroscopy instead of CEA).

As the spectral information is deduced from the time-integrated signal rather than from the time dependence of the signal, it is possible to perform these measurements with relative low-power lasers and cheap detection systems. Combined with the sensitivity of CEA spectroscopy, trace gas detection based on the CEA technique might offer attractive possibilities.

Recently, we have developed a compact open-path ammonia detector which uses a commercially available ECDL operating at 1.5 μm (Peeters *et al.* 2000). The set-up

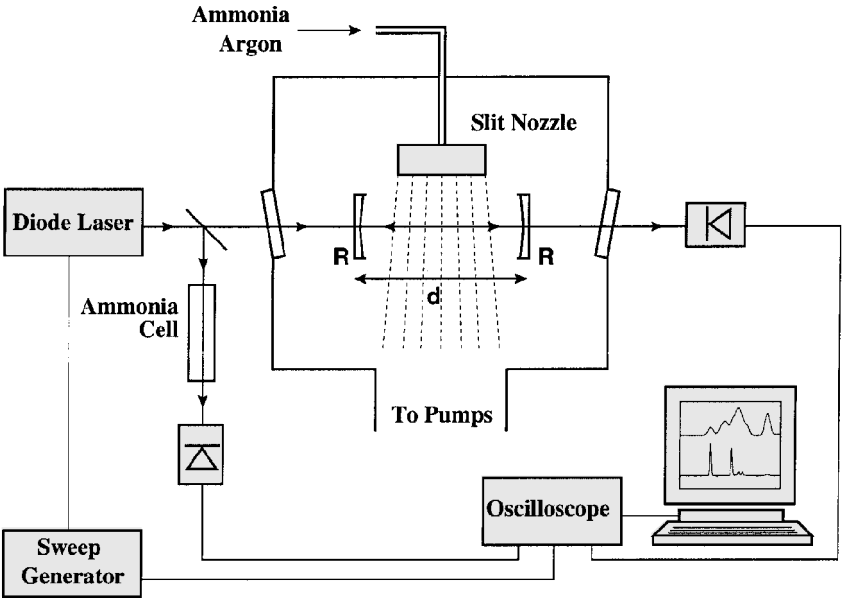

Figure 9. Experimental set-up for recording the CEA spectra of jet-cooled ammonia. The wavelength of the CW diode laser is scanned over 1 cm^{-1} at a rate of 30 Hz using a sweep generator, which also triggers the data acquisition. Part of the laser beam is used to record the absorption spectrum of ammonia at room temperature. Light is coupled into the high-finesse optical cavity 8·5 cm long, which is enclosed in a vacuum chamber. The vacuum chamber is evacuated by a 1200 $m^3\ h^{-1}$ Roots pump backed by a 180 m^3 rotary pump. A planar jet is formed by expanding ammonia strongly diluted in argon through a 40 mm $\times$ 0·03 mm slit nozzle. The cavity axis is along the long axis of the slit nozzle, intersecting the jet a few millimetres downstream from the orifice. The light that leaks out of the cavity is detected with a photodiode and displayed on the oscilloscope, which is used in x–y mode. The horizontal axis is triggered by the sweep generator and is therefore proportional to the laser wavelength. Further data analysis is performed on a PC. (Figure reproduced from Berden *et al.* (1999) with permission. Copyright Elsevier Science.)

consists of a diode laser, a high-finesse cavity (R = 0·9997) with one mirror mounted on a piezoelectric transducer used to vary the cavity length, and a (slow) photodiode. Data acquisition was carried out with an analogue-to-digital card and Labview-based software. The system was tested in a climate chamber, where it was possible to vary the amount of ammonia and water in the air. Figure 8 gives an overview of the results. The ammonia and water concentrations were calibrated independently using a chemiluminescence monitor and a relative humidity monitor respectively. It is concluded that the CEA signal is indeed linear with the concentration of the molecules. Furthermore, these measurements show that the sensitivity for detection of ammonia under atmospheric pressure is 2×10^{-8} cm^{-1}.

The spectral width of spectroscopic features in figures 7 and 8 are dominated by Doppler broadening and pressure broadening respectively, while the bandwidth of the lasers is less than 5 MHz (10^{-4} cm^{-1}). The high-resolution character of CEA spectroscopy has been demonstrated by recording absorption spectra of oxygen (Engeln *et al.* 1998) and ammonia (Berden *et al.* 1999) in a molecular jet. The experimental set-up which is used to record the spectra of ammonia is shown in figure 9. Jet-cooled spectra of ammonia are shown in figure 10. The FWHM of the rotational transitions is 180 MHz, demonstrating the high-resolution character of CEA

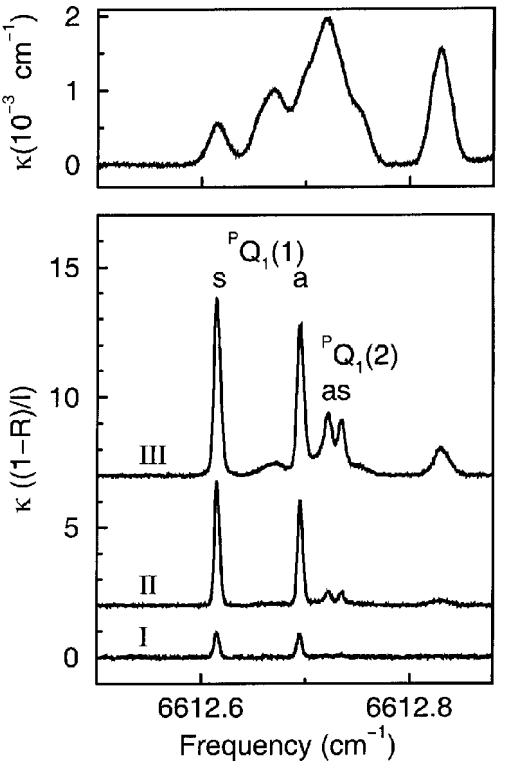

Figure 10. Part of the $\nu_1+\nu_3$ spectrum of ammonia containing the $^{P}Q_1$ branch. The lower part shows the CEA spectra recorded in a jet obtained by seeding different amounts of ammonia in argon. The ammonia concentration increases from spectrum I to III. The absorption coefficient κ is expressed in units of $(1-R)/l$ which is about 1×10^{-4} cm^{-1}. Spectra II and III have been offset for clarity. The upper part shows the corresponding part of the single-pass absorption spectrum of ammonia at 3 mbar and room temperature. (Figure reproduced from Berden *et al.* (1999) with permission. Copyright Elsevier Science).

spectroscopy. Mechanical vibrations due to the pumps did not perturb the measurements; on the contrary, they introduce a randomization of the jittering of the cavity length which in turn increases the in-coupling efficiency of the laser light and thereby the signal-to-noise ratio of the spectrum.

A different way of performing CEA spectroscopy has been reported by He and Orr (2000). They have constructed a cavity in such a way that the cavity will exhibit a dense mode structure, with the modes at isolated frequencies. In addition to the cavity decay time, as has already been mentioned before (section 3), they have measured the CEA peak signal instead of the *total* time-integrated cavity signal. In their experiment they only allowed for a short resonance time, resulting in a short intracavity intensity build-up and a longer decay time. The CEA signal was now derived by integrating the intensity in a narrow gate around the maximum intracavity intensity. They compared the sensitivity achieved with this 'peak-detected' CEA scheme with the sensitivity obtained with the CW-CRD scheme. They remarked that the baseline noise level in the CW-CRD experiments is better than in the 'peak-detected' CEA spectra and assigned this to power fluctuations in the laser output and spatial and wavelength instabilities of the laser. However, it is obvious that, in using 'peak-detected' CEA spectroscopy,

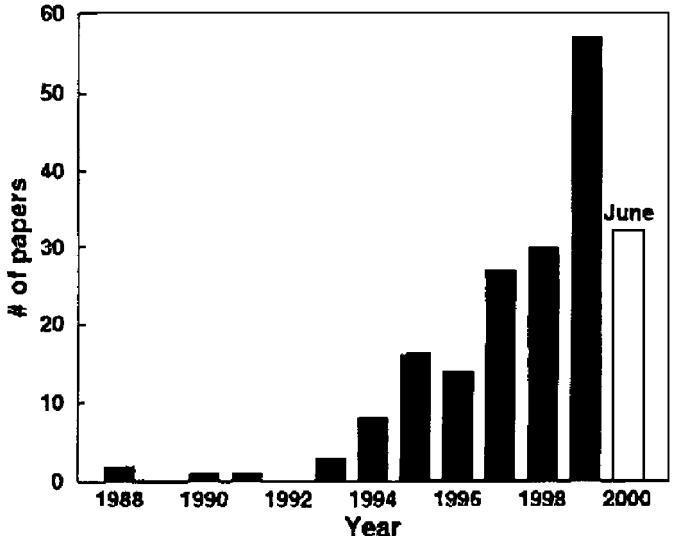

Figure 11. The number of papers on CRD spectroscopy as a function of the year of appearance.

one does not fully exploit the effective measurement path length achievable in the high-finesse optical cavity. Therefore, the attainable sensitivity does not compare with the sensitivity of pulsed CRD, CW-CRD or CEA spectroscopy.

The CEA technique can also be used to measure optical rotation spectra, by placing a polarization analyser in front of the detector (Engeln *et al.* 1998). This cavity-enhanced magnetic rotation (CEMR) scheme is closely related to the PD-CRD scheme (see section 2.6.2). The experimental set-up for CEMR is slightly different from the CEA set-up. Prior to entering the optical cavity the laser beam passes through a polarizer to define the polarization state of the incoming light better. A second polarizer, which is set at an angle of ϕ_D relative to the polarization of the incoming light, is placed in front of the detector which measures the time integrated intensity. For $\phi_D = 90°$, the recorded spectrum is a result of optical polarization rotation due to magnetic birefringence while, for ϕ_D away from 90°, the spectrum is dominated by magnetic dichroism.

It is clear that the CEA technique is an addition to the pulsed and CW-CRD techniques. An attractive feature of CEA spectroscopy is the simple experimental set-up combined with a good sensitivity. The ultimate sensitivity is limited by the residual mode structure and power fluctuations of the laser and is therefore not as good as can be achieved with CRD spectroscopy.

5. Applications

By now (June 2000), more than 190 papers on CRD spectroscopy have appeared. Figure 11 shows the number of CRD papers as a function of the year of appearance (the numbers are taken from the reference list of this paper). It is evident that CRD spectroscopy is becoming a standard spectroscopic tool. This conclusion can also be drawn by looking at the titles of the papers; more and more papers appear with titles *without* the words 'cavity ring-down'.

Table 1. Overview of the CRD literature (June 2000).

Wavelength (nm)	Molecule	Technique[a]	t, s, d[b]	Environment	References
205	NH_3	Pulsed CRD	d	Cell	Jongma *et al.* (1995)
206	CO	Pulsed CRD	s	Cell	Jongma *et al.* (1994)
214	CH_3	Pulsed CRD	d	Hot-filament reactor	Wahl *et al.* (1996, 1997)
215–233	CF	Pulsed CRD	s, d	Etching plasma reactor	Booth *et al.* (2000)
216	CH_3	Pulsed CRD	d	Hot-filament reactor	Zalicki *et al.* (1995a, 1995b)
220–222	C_2H_5	Pulsed CRD	d	Laser photolysis reactor	Atkinson and Hudgens (1997)
221	SiF_2	Pulsed CRD	s, d	Etching plasma reactor	Booth *et al.* (2000)
225–238	C_2H_3	Pulsed CRD	s	Laser photolysis reactor	Fahr *et al.* (1998)
227	AlF	Pulsed CRD	s, d	Etching plasma reactor	Booth *et al.* (2000)
237	CF_2	Pulsed CRD	s, d	Etching plasma reactor	Booth *et al.* (2000)
238–252	C_3H_3X, X = Cl_2, ClBr, Br_2	Pulsed CRD	s, d	Laser photolysis reactor	Atkinson and Hudgens (1999b)
238–252	C_3H_4Cl	Pulsed CRD	s, d	Laser photolysis reactor	Atkinson and Hudgens (2000)
242–244	O_2	Pulsed CRD	s	Cell	Slanger *et al.* (1996)
243–258	O_2	Pulsed CRD	s	Cell	Huestis *et al.* (1994)
245–253	OH	Pulsed CRD	s	Atmospheric laminar CH_4–air flame	Spaanjaars *et al.* (1997)
250–282	S_2	Pulsed CRD	s	Flow reactor	Wheeler *et al.* (1998b)
254	Hg	Pulsed CRD	d	Open air	Jongma *et al.* (1995)
254	Hg	Pulsed CRD	d	Cell	Spuler *et al.* (2000)
254	Hg	Pulsed CRD	d	Cell; open air	Tao *et al.* (2000)
265–270	$C_2H_5O_2$	Pulsed CRD	d	Laser photolysis reactor	Atkinson and Hudgens (1997)
265–340	$C_2H_5ONO_2$	Pulsed CRD	s, d	Laser photolysis reactor	Zhu and Ding (1997)
265–340	$C_nH_{2n+1}ONO_2$, n = 2–5	Pulsed CRD	s, d	Laser photolysis reactor	Zhu and Kellis (1997)
266	C_6H_5Cl, $C_6H_4Cl_2$	Pulsed CRD	d	Cell	Vasudev *et al.* (1999)
279–306	HClCO	Pulsed CRD	s	Cell	Ding *et al.* (1999)
280	Mg^+	Pulsed CRD	d	Inductively coupled plasma	Miller and Winstead (1997)
283	Pb	Pulsed CRD	d	Inductively coupled plasma	Miller and Winstead (1997)
283	Pb	Pulsed CRD	d	Graphite furnace	Winstead *et al.* (1999)
287–320	ClO	Pulsed CRD	s	Cell	Howie *et al.* (1999)
298	OH	Pulsed CRD	d	Atmospheric CH_4–air flame	Meijer *et al.* (1994)
298–317	SH, SD	Pulsed CRD	s	Flow reactor	Wheeler *et al.* (1997a)
306	SH	Pulsed CRD	s	Flow reactor	Wheeler *et al.* (1997b)

Table 1. (*cont.*)

Wavelength (nm)	Molecule	Technique[a]	t, s, d[b]	Environment	References
308	OH	Pulsed CRD	d	Open air (heated)	Jongma *et al.* (1995)
308	OH	Pulsed CRD	d	Low-pressure CH_4–air flame	Cheskis *et al.* (1998)
308	OH	Pulsed CRD	d	Atmospheric flames	Mercier *et al.* (1999b)
308	$(C_6H_5)_2NH$	Pulsed CRD	s	Pulsed jet; laser desorption	Boogaarts and Meijer (1995)
310–330	CH_2CCH	Pulsed CRD	s, d	Laser photolysis reactor	Atkinson and Hudgens (1999a)
312	OH	Pulsed CRD	d	Low-pressure CH_4–air flame	Lozovsky *et al.* (1998)
315	CH	Pulsed CRD	d	Atmospheric flames	Mercier *et al.* (1999a)
315	CH	Pulsed CRD	d	Low-pressure CH_4–air flame	Derzy *et al.* (1999b)
316–339	BrO	Pulsed CRD	s	Flow reactor	Wheeler *et al.* (1998a)
330–350	C_2H_3O	Pulsed CRD	s, d	Laser photolysis reactor	Zhu and Johnston (1995)
334	NH	Pulsed CRD	d	Low-pressure CH_4–NO–air flame	Derzy *et al.* (1999a)
334–379	C_4	Pulsed CRD	s	Pulsed jet; slit nozzle discharge	Linnartz *et al.* (2000)
337–362	PtSi	Pulsed CRD	s	Pulsed jet; laser vaporization	Paul *et al.* (1996)
339	BrO	Pulsed CRD	d	Laser photolysis reactor	Ninomiya *et al.* (2000)
340	Cl_2	Pulsed CRD	d	Laser photolysis reactor	Atkinson and Hudgens (1997)
340–390	AuSi	Pulsed CRD	s	Pulsed jet; laser vaporization	Scherer *et al.* (1995a)
355	Aerosols	Pulsed CRD	d	Cell; Mie scattering	Sappey *et al.* (1998)
365–385	AgSi	Pulsed CRD	s	Pulsed jet; laser vaporization	Scherer *et al.* (1995c)
380–410	CuSi	Pulsed CRD	s	Pulsed jet; laser vaporization	Scherer *et al.* (1995b)
385	NaH	Pulsed CRD	s	Heat-pipe oven	Lehr and Hering (1997a, b)
404–412	Al_2	Pulsed CRD	s	Pulsed jet; laser vaporization	Scherer *et al.* (1995e)
415–530	C_2H_3	Pulsed CRD	s	Laser photolysis reactor	Pibel *et al.* (1999)
418–470	IO	Pulsed CRD	s	Flow reactor	Newman *et al.* (1998)
427	WO	Pulsed CRD	s	Pulsed jet; laser vaporization	Kraus *et al.* (1998)
430	CH	Pulsed CRD	d	Atmospheric flames	Evertsen *et al.* (1999, 2000)
430	CH	Pulsed CRD	d	Diamond depositing flame	Stolk and Ter Meulen (1999)
430	CH	Pulsed CRD	d	Expanding Ar–C_2H_2 plasma	Engeln *et al.* (1999a)
430	CH	Pulsed CRD	d	Low-pressure CH_4–O_2–Ar flame	Thoman and McIlroy (2000)
431	CH	Pulsed CRD	d	Hot-filament reactor	Lommatzsch *et al.* (2000)
435–571	HCN	Pulsed CRD	s	Cell	Romanini and Lehmann (1993, 1996b)
435–571	HCN, $H^{13}CN$, $HC^{15}N$	Pulsed CRD	s	Cell	Romanini and Lehmann (1996, 1996a)

Table 1. (*cont.*)

Wavelength (nm)	Molecule	Technique[a]	t, s, d[b]	Environment	References
436–442	C_2H_2O	Pulsed CRD	s, d	Laser photolysis reactor	Zhu and Johnston (1995)
438–452	NO_2	Pulsed CRD	d	Laser photolysis reactor	Zhu and Kellis (1997)
444–455	C_2H_3	Pulsed CRD	s	Laser photolysis reactor	Tonokura *et al.* (1999)
445–458	IO	Pulsed CRD	d	Laser photolysis reactor	Atkinson *et al.* (1999)
453	Cu_2	Pulsed CRD	s	Pulsed jet; laser vaporization	O'Keefe *et al.* (1990)
459	HC_7H	Pulsed CRD	s	Pulsed jet; slit nozzle discharge	Ball *et al.* (2000)
460	Cr_2	Pulsed CRD	s	Pulsed jet; laser vaporization	Kraus *et al.* (1999)
471	BiF	Pulsed CRD	d	Chemical reactor	Benard and Winker (1991)
490–512	C_5	Pulsed CRD	s	Pulsed jet; slit nozzle discharge	Motylewski *et al.* (1999)
496	$C_6H_5O_2$	Pulsed CRD	d	Laser photolysis reactor	Yu and Lin (1994b)
496–530	C_6H_5	Pulsed CRD	s, d	Laser photolysis reactor	Yu and Lin (1994b)
504	HC_7H	Pulsed CRD	s	Pulsed jet; slit nozzle discharge	Ball *et al.* (1999, 2000)
505	C_6H_5	Pulsed CRD	d	Laser photolysis reactor	Yu and Lin (1993, 1994a, 1994d, 1995a, 1995b)
505	C_6H_5	Pulsed CRD	d	Laser photolysis reactor	Lin and Yu (1993)
505	C_6H_5	Pulsed CRD	d	Laser photolysis reactor	Park *et al.* (1999a, 1999c)
505	C_6H_5	Pulsed CRD	d	Laser photolysis reactor	Nam *et al.* (2000)
505	N_2^+	Pulsed CRD	s	Hollow cathode discharge cell	Kotterer *et al.* (1996)
505–602	C_6H_5O	Pulsed CRD	d	Laser photolysis reactor	Yu *et al.* (1995)
508	C_6H_5	Pulsed CRD	d	Laser photolysis reactor	Park *et al.* (1999b)
510	$C_6H_5O_2$	Pulsed CRD	d	Laser photolysis reactor	Yu and Lin (1994c)
522	HC_9H	Pulsed CRD	s	Pulsed jet; slit nozzle discharge	Ball *et al.* (1999, 2000)
526	C_6H, C_6D	Pulsed CRD	s	Hollow cathode discharge cell	Kotterer and Maier (1997)
526	C_6H	Pulsed CRD	t	Pulsed jet; slit nozzle discharge	Motylewski and Linnartz (1999)
526	C_6H, C_6D	Pulsed CRD	s	Pulsed jet; slit nozzle discharge	Linnartz *et al.* (1999)
532	H^-	Pulsed CRD	d	Discharge plasma (photodetachment)	Quandt *et al.* (1998)
532	Aerosols	Pulsed CRD	d	Cell; Mie scattering	Sappey *et al.* (1998)
532	Soot	Pulsed CRD	d	CH_4–air flames	Vander Wal and Ticich (1999)
532	Grating	Pulsed CRD	d	Detection of laser-induced grating	Hemmerling and Kozlov (1999)
538	NH_2	Pulsed CRD	d	Laser photolysis NH_3	Diau *et al.* (1994)
538	NH_2	Pulsed CRD	d	Laser photolysis NH_3	Yu and Lin (1994a)
538	C_2^-	Pulsed CRD	s, d	Pulsed jet; slit nozzle discharge	Motylewski and Linnartz (1999)

Table 1. (*cont.*)

Wavelength (nm)	Molecule	Technique[a]	t, s, d[b]	Environment	References
540	Cu_3	Pulsed CRD	s	Pulsed jet; laser vaporization	O'Keefe *et al.* (1990)
540	I_2	EW-CRD	t	Molecules at surface	Pipino (2000)
540–575	Cl_2CS	Pulsed CRD	s	Pulsed jet	Moule *et al.* (1999)
540–650	HNO	Pulsed CRD	s	Cell	Pearson *et al.* (1996, 1997)
540–650	$(O_2)_2$	Pulsed CRD	s	Cell	Naus and Ubachs (1999b)
540–650	Ar, N_2, SF_6	Pulsed CRD	s	Cell; Rayleigh extinctions	Naus and Ubachs (2000)
552–627	C_8H, C_8D	Pulsed CRD	s	Pulsed jet; slit nozzle discharge	Linnartz *et al.* (1998)
562–582	NO_2	Pulsed CRD	d	Cell	Vasudev *et al.* (1999)
566	O^-, H^-	Pulsed CRD	d	Rf plasma reactor (photodetachment)	Grangeon *et al.* (1999)
566	Particles	Pulsed CRD	d	Rf plasma reactor (scattering)	Grangeon *et al.* (1999)
570	C_2H_2	CW-CRD	t	Cell	Romanini *et al.* (1997a)
570	C_2H_2	CW-CRD	t, d	Cell	Hahn *et al.* (1999)
575–705	Asulene	Pulsed CRD	s	Pulsed jet	Ruth *et al.* (1999)
579	SiH_2	CW-CRD	s, d	Discharge cell	Campargue *et al.* (1998)
580	$^xO^yO$	Pulsed CRD	s	Cell	Naus and Ubachs (1999a)
580	I_2	EW-CRD	t	Molecules at surface	Pipino (1999)
580	$HC_{11}H$	Pulsed CRD	s	Pulsed jet; slit nozzle discharge	Ball *et al.* (2000)
582	HC_9H	Pulsed CRD	s	Pulsed jet; slit nozzle discharge	Ball *et al.* (1999, 2000)
600	$C_6H_2^+, C_6D_2^+, HC_6D^+$	Pulsed CRD	s, d	Pulsed jet; slit nozzle discharge	Motylewski and Linnartz (1999)
600–620	H_2O_2	Pulsed CRD	s	Cell	Brown *et al.* (2000)
600–633	C_7H_6SO	Pulsed CRD	s	Pulsed jet	Ruth *et al.* (1998)
604	C_6H_6	Pulsed CRD	s	Heated cell	Kleine *et al.* (1999)
611	N_2^+	Pulsed CRD	d	Hollow cathode discharge cell	Kotterer *et al.* (1996)
615	HCO	Pulsed CRD	d	Laser photolysis glyoxal	Zhu *et al.* (1996)
615	HCO	Pulsed CRD	s, d	Low-pressure CH_4–N_2–O_2 flame	Scherer and Rakestraw (1997)
615	HCO	Pulsed CRD	d	Low-pressure CH_4 flame	McIlroy (1999)
615	HCO	Pulsed CRD	d	Laser photolysis reactor	Cronin and Zhu (1998)
615	HCO	Pulsed CRD	d	Laser photolysis reactor	Zhu *et al.* (1999)
615	HCO	Pulsed CRD	d	Laser photolysis reactor	Min *et al.* (1999)
615	HCO	Pulsed CRD	d	Laser photolysis reactor	Zhu and Cronin (2000)
615–621	HNO_3	Pulsed CRD	s	Cell	Brown *et al.* (2000)

Table 1. (*cont.*)

Wavelength (nm)	Molecule	Technique[a]	t, s, d[b]	Environment	References
620–715	$C_{10}H, C_{10}D$	Pulsed CRD	s	Pulsed jet; slit nozzle discharge	Linnartz *et al.* (1998)
622	CH_2	Pulsed CRD	d	Low-pressure CH_4–O_2–Ar flame	McIlroy (1998)
625	I_2	EW-CRD	t	Cell	Pipino *et al.* (1997b)
625–645	$CH_3CH_2CH_3$	RSP	t	Cell	Scherer (1998)
627–635	N_2^+	Pulsed CRD	s	Hollow cathode discharge cell	Aldener *et al.* (2000)
628	O_2	Pulsed CRD	t	Cell; open air	O'Keefe and Deacon (1988)
628	O_2	CEA	t	Cell	Engeln *et al.* (1998)
629	O_2	PD-CRD	t	Cell	Engeln *et al.* (1997a)
629	O_2	CEMR	t	Cell	Engeln *et al.* (1998)
630	$^xO^yO$	Pulsed CRD	s	Cell	Naus *et al.* (1999)
630	O_2	Pulsed CRD	s, d	Cell	Xu *et al.* (1999)
630	I_2	Pulsed CRD	t	Cell	Meijer *et al.* (1994)
632	$(O_2)_2$	CW-CRD	s	Continuous jet	Biennier *et al.* (2000)
635	$^{18}O_2$	PS-CRD	t, s	Cell	Engeln *et al.* (1996)
639	CH_3CCH	Pulsed CRD	s	Cell	Campargue *et al.* (1999)
639	Li_2	Pulsed CRD	s	Heat-pipe oven	Labazan *et al.* (2000)
645–680	$C_{10}H_8^+$	Pulsed CRD	s	Pulsed jet; slit nozzle discharge	Romanini *et al.* (1999a)
654	$HC_{11}H$	Pulsed CRD	s	Pulsed jet; slit nozzle discharge	Ball *et al.* (2000)
655–670	NO_3	CW-CRD	d	Cell; open air	King *et al.* (2000)
656	H	Pulsed CRD	d	Expanding Ar–C_2H_2 plasma	Van de Sanden *et al.* (1999)
659	H_2O	CW-CRD	t	Open air	Schulz and Simpson (1998)
688	O_2	Pulsed CRD	t	Cell; open air	O'Keefe and Deacon (1988)
688	O_2	Pulsed CRD	s	Cell	Seiser and Robie (1998)
688	$^xO^yO$	Pulsed CRD	s	Cell	Naus *et al.* (1998)
690	O_2	Pulsed CRD	t	Cell	O'Keefe (1998)
690	O_2	Pulsed CRD	s	Cell	Xu *et al.* (1999)
718	$HC_{13}H$	Pulsed CRD	s	Pulsed jet; slit nozzle discharge	Ball *et al.* (2000)
730–755	H_2O_2	Pulsed CRD	s	Cell	Brown *et al.* (2000)
752–758	HNO_3	Pulsed CRD	s	Cell	Brown *et al.* (2000)
762	O_2	FT-CRD	t	Cell	Engeln and Meijer (1996)
762	$^xO^yO$	Pulsed CRD	s	Cell	Naus *et al.* (1997)

Table 1. (*cont.*)

Wavelength (nm)	Molecule	Technique[a]	t, s, d[b]	Environment	References
762	O_2	Pulsed CRD	s, t	Cell in high magnetic field	Berden *et al.* (1998)
762	O_2	CEA	t	Continuous jet	Engeln *et al.* (1998)
764	O_2	Pulsed CRD	s, d	Cell	Xu *et al.* (1999)
765	O_2	Pulsed CRD	t	Cell	Hodges *et al.* (1996a)
765	O_2	Pulsed CRD	t	Cell	Van Zee *et al.* (1999)
770–778	CHF_3	CW-CRD	s	Cell	Romanini *et al.* (1997c)
776	N_2O	CW-CRD	t	Cell	Romanini *et al.* (1997b)
785	NO_2	CW-CRD	t	Continuous jet	Romanini *et al.* (1997b)
797	NO_2	CW-CRD	s	Continuous jet	Romanini *et al.* (1999b)
812–819	H_2O	Pulsed CRD	d, s	Atmospheric flames	Xie *et al.* (1998)
813	H_2O	CW-CRD	t	Cell	Paldus *et al.* (1997)
834	H_2O	CW-CRD	t	Open air	Paldus *et al.* (1998)
834	H_2O	CW-CRD	t	Open air	Levenson *et al.* (1998)
1032	C_2H_2	CW-CRD	t	Cell	Ye and Hall (2000)
1064	CO_2	CW-CRD	d	Cell	Inbar and Arie (1999)
1064	C_2H_2	CW-CRD	d	Cell	Inbar and Arie (1999)
1064	CO_2	CW-CRD	t	Cell	Spence *et al.* (2000)
1064	CO_2	CW-CRD	t	Cell	Levenson *et al.* (2000)
1102	H_2O	Pulsed CRD	d	Cell	Ramponi *et al.* (1988)
1270	O_2	Pulsed CRD	s	Cell	Newman *et al.* (1999)
1285	N_2O	CW-CRD	t	Cell	He *et al.* (1998)
1285	N_2O	CW-CRD	t	Pulsed jet	Hippler and Quack (1999)
1295	$CHCl_3$	CW-CRD	s	Cell	He *et al.* (1998)
1299–1370	CH_3O_2	Pulsed CRD	s	Laser photolysis reactor	Pushkarsky *et al.* (2000)
1299–1333	$C_2H_5O_2$	Pulsed CRD	s	Laser photolysis reactor	Pushkarsky *et al.* (2000)
1320	CO_2	CEA	t	Cell	O'Keefe *et al.* (1999)
1327	H_2O	CEA	d	Cell	O'Keefe *et al.* (1999)
1331	CH_4	CW-CRD	s	Pulsed jet	Hippler and Quack (1999)
1391	CH_3OH	CW-CRD	d	Cell	Totschnig *et al.* (2000)
1402	$(CH_3)_2CHOH$	CW-CRD	d	Cell	Totschnig *et al.* (2000)
1508–1563	NH_3	CEA	s	Continuous jet	Berden *et al.* (1999)
1509	OH, H_2O	Pulsed CRD	d	Low-pressure H_2–O_2 flame	Scherer *et al.* (1997c)
1518	NH_3	CEA	t	Cell	Engeln *et al.* (1998)
1518	H_2O	CEA	d	Open air	Peeters *et al.* (2000)

Table 1. (*cont.*)

Wavelength (nm)	Molecule	Technique[a]	t, s, d[b]	Environment	References
1522	NH_3	CEA	d	Open air	Peeters *et al.* (2000)
1538	CO_2	CW-CRD	t	Cell	He and Orr (2000)
1547	C_2H_2	Pulsed CRD	d	Cell	Scherer *et al.* (1995f)
1769	$(HCl)_2$	Pulsed CRD	s	Pulsed jet	Liu *et al.* (1998)
2630–3330	$(H_2O)_n$, n = 2–8	Pulsed CRD	s	Pulsed jet	Paul *et al.* (1997)
2700–3280	$(CH_3OH)_n$, n = 2–4	Pulsed CRD	s	Pulsed jet	Provencal *et al.* (1999)
2700–3570	$(CH_3CH_2OH)_n$, n = 2–4	Pulsed CRD	s	Pulsed jet	Provencal *et al.* (2000)
2700–3570	$(CH_3(CH_2)_3OH)_n$, n = 2–4	Pulsed CRD	s	Pulsed jet	Provencal *et al.* (2000)
3100–3170	CH_3	Pulsed CRD	d	Low-pressure CH_4–air flame	Scherer *et al.* (1997a)
3161	CH_4, C_2H_2, H_2O	Pulsed CRD	d	Low-pressure flame	Scherer *et al.* (1997c)
3290–3570	$(HCOOH)_2$	Pulsed CRD	s	Pulsed jet	Ito and Nakanaga (2000)
3311	CH_{42}	Pulsed CRD	t	Cell	Aniolek *et al.* (1999)
3315	CH_4	Pulsed CRD	d, t	Cell	Scherer *et al.* (1995f)
3570–3610	$(D_2O)_2$	Pulsed CRD	s	Pulsed jet	Paul *et al.* (1998b)
3570–4350	$(D_2O)_n$, n = 2–8	Pulsed CRD	s	Pulsed jet	Paul *et al.* (1998a)
5381	H_2O	Pulsed CRD	t	Cell (pulsed stacked CRD)	Crosson *et al.* (1999)
5710–6450	Arginine	Pulsed CRD	s	Pulsed jet	Chapo *et al.* (1998)
5990–6340	$(H_2O)_n$, n = 2–4	Pulsed CRD	s	Pulsed jet	Paul *et al.* (1999)
8460	C_{60}	Pulsed CRD	t, s	Thin solid film	Engeln *et al.* (1999b)
8496	NH_3	CW-CRD	t	Cell	Paldus *et al.* (2000)
10190–10690	C_2H_4	CW-CRD	d	Cell	Mürtz *et al.* (1999)
10530	C_2H_4	Pulsed CRD	t	Cell	Engeln *et al.* (1997b)
10530	C_2H_4	FT-CRD	t	Cell	Engeln *et al.* (1997b)
10617	C_2H_4	CW-CRD	t, s	Cell	Bucher *et al.* (2000)

[a] Pulsed CRD, pulsed cavity ring-down spectroscopy; EW-CRD, evanescent wave cavity ring-down spectroscopy, CW-CRD, continuous-wave cavity ring-down spectroscopy; RSP, ring-down spectral photography; CEA, cavity-enhanced absorption spectroscopy; PD-CRD, polarization-dependent cavity ring-down spectroscopy; CEMR, cavity-enhanced magnetic rotation spectroscopy; PS-CRD, phase-shift cavity ring-down spectroscopy; FT-CRD, Fourier transform cavity ring-down spectroscopy.

[b] t, study describing a technique; s, spectroscopic study; d, CRD technique used for trace gas detection.

Since this review is focused on the various experimental schemes of CRD spectroscopy, we shall only briefly mention the applications of CRD spectroscopy. Table 1 gives an overview of the literature. Care has been taken to make this table as complete as possible but, nevertheless, there might be papers that have escaped our attention.

Although the papers are listed according to the wavelength used in the reported studies, they can be categorized in three groups. The first group (labelled *t*) contains those papers which describe a particular CRD scheme and contain CRD spectra demonstrating the specific technique. Papers reporting a spectroscopic study of a molecular system, belong to the second group (labelled *s*), while papers which use CRD spectroscopy for the detection of species in a certain environment are in the third group (labelled *d*).

From this table, several conclusions can be drawn. First of all, CRD spectroscopy has been performed in quite a large spectral region, from the UV (200 nm) to the IR (10 μm), almost without gaps. Second, a large variety of atoms and molecules have been studied, including radicals, ions, clusters and even molecules in the solid phase. Besides the detection of molecular absorptions, the technique has also been used to measure extinctions due to, for example, scattering and photodetachment. Third, CRD spectroscopy can be applied in many environments; in open air, cells, jets, discharges and flames.

Very generally, one can say that reported detection sensitivies for all CRD schemes are in the 10^{-6}–10^{-10} cm^{-1} range for multimode excitation of the ring-down cavity, and in the 10^{-9}–10^{-12} cm^{-1} range for single-mode excitation. This good sensitivity combined with a fairly simple experimental set-up, makes these direct absorption techniques very powerful in many areas of research.

Acknowledgments

We are very grateful to our many colleagues in Nijmegen who have contributed in important ways to the CRD experiments that are highlighted in this review, especially Richard Engeln, Rienk Jongma, Maarten Boogaarts, Iwan Holleman, Hans Naus, Esther van den Berg, Gert von Helden and André van Roij. This work is financially supported by the Nederlandse Organisatie voor Wetenschappelijk Onderzoek.

References

Aldener, M., Lindgren, B., Pettersson, A., and Sassenberg, U., 2000, *Physica scripta*, **61**, 62.
An, K., Yang, C., Dasari, R. R., and Feld, M. S., 1995, *Optics Lett.*, **20**, 1068.
Anderson, D. Z., Frisch, J. C., and Masser, C. S., 1984, *Appl. Optics*, **23**, 1238.
Aniolek, K. W., Powers, P. E., Kulp, T. J., Richman, B. A., and Bisson, S. E., 1999, *Chem. Phys. Lett.*, **302**, 555.
Atkinson, D. B., and Hudgens, J. W., 1997, *J. phys. Chem.* A, **101**, 3901; 1999a, *ibid.*, **103**, 4242; 1999b, *ibid.*, **103**, 7978; 2000, *ibid.*, **104**, 811.
Atkinson, D. B., Hudgens, J. W., and Orr-Ewing, A. J., 1999, *J. phys. Chem.* A, **103**, 6173.
Ball, C. D., McCarthy, M. C., and Thaddeus, P., 1999, *Astrophys. J.*, **523**, L89; 2000, *J. chem. Phys.*, **112**, 10149.
Benard, D. J., and Winker, B. K., 1991, *J. appl. Phys.*, **69**, 2805.
Berden, G., Engeln, R., Christianen, P. C. M., Maan, J. C., and Meijer, G., 1998, *Phys., Rev.* A, **58**, 3114.
Berden, G., Peeters, R., and Meijer, G., 1999, *Chem. Phys. Lett.*, **307**, 131.
Biennier, L., Romanini, D., Kachanov, A., Campargue, A., Bussery-Honvault, B., and Bacis, R., 2000, *J. chem. Phys.*, **112**, 6309.
Boogaarts, M. G. H., and Meijer, G., 1995, *J. chem. Phys.*, **103**, 5269.

BOOTH, J. P., CUNGE, G., BIENNIER, L., ROMANINI, D., and KACHANOV, A., 2000, *Chem. Phys. Lett.*, **317**, 631.
BROWN, S. S., WILSON, R. W., and RAVISHANKARA, A. R., 2000, *J. phys. Chem.* A, **104**, 4976.
BUCHER, C. R., LEHMANN, K. K., PLUSQUELLIC, D. F., and FRASER, G. T., 2000, *Appl. Optics*, **39**, 3154.
BUSCH, K. W., and BUSCH, M. A. (editors), 1999, *Cavity-Ringdown Spectroscopy, An Ultratrace-Absorption Measurement Technique*, ACS Symposium Series 720 (Washington, DC: American Chemical Society).
CAMPARGUE, A., BIENNIER, L., GARNACHE, A., KACHANOV, A., ROMANINI, D., and HERMAN, M., 1999, *J. chem. Phys.*, **111**, 7888.
CAMPARGUE, A., ROMANINI, D., and SADEGHI, N., 1998, *J. Phys.* D, **31**, 1168.
CHAPO, C. J., PAUL, J. B., PROVENCAL, R. A., ROTH, K., and SAYKALLY, R. J., 1998, *J. Am. chem. Soc.*, **120**, 12956.
CHESKIS, S., 1999, *Prog. Energy Combust. Sci.*, **25**, 233.
CHESKIS, S., DERZY, I., LOZOVSKY, V. A., KACHANOV, A., and ROMANINI, D., 1998, *Appl. Phys.* B, **66**, 377.
CRONIN, T. J., and ZHU, L., 1998, *J. phys. Chem.* A, **102**, 10274.
CROSSON, E. R., HAAR, P., MARCUS, G. A., SCHWETTMAN, H. A., PALDUS, B. A., SPENCE, T. G., and ZARE, R. N., 1999, *Rev. scient. Instrum.*, **70**, 4.
DERZY, I., LOZOVSKY, V. A., and CHESKIS, S., 1999a, *Isr. J. Chem.*, **39**, 49; 1999b, *Chem. Phys. Lett.*, **306**, 319.
DIAU, E. W., YU, T., WAGNER, M. A. G., and LIN, M. C., 1994, *J. phys. Chem.*, **98**, 4034.
DING, H., ORR-EWING, A. J., and DIXON, R. N., 1999, *Phys. Chem. chem. Phys.*, **1**, 4181.
ENGELN, R., BERDEN, G., PEETERS, R., and MEIJER, G., 1998, *Rev. scient. Instrum.*, **69**, 3763.
ENGELN, R., BERDEN, G., VAN DEN BERG, E., and MEIJER, G., 1997a, *J. chem. Phys.*, **107**, 4458.
ENGELN, R., LETOURNEUR, K. G. Y., BOOGAARTS, M. G. H., VAN DE SANDEN, M. C. M., and SCHRAM, D. C., 1999a, *Chem. Phys. Lett.*, **310**, 405.
ENGELN, R., and MEIJER, G., 1996, *Rev. scient. Instrum.*, **67**, 2708.
ENGELN, R., VAN DEN BERG, E., MEIJER, G., LIN, L., KNIPPELS, G. M. H., and VAN DER MEER, A. F. G., 1997b, *Chem. Phys. Lett.*, **269**, 293.
ENGELN, R., VON HELDEN, G., BERDEN, G., and MEIJER, G., 1996, *Chem. Phys. Lett.*, **262**, 105.
ENGELN, R., VON HELDEN, G., VAN ROIJ, A. J. A., and MEIJER, G., 1999b, *J. chem. Phys.*, **110**, 2732.
EVERTSEN, R., STOLK, R. L., and TER MEULEN, J. J., 1999, *Combust. Sci. Technol.*, **149**, 19; 2000, *ibid.*, **157**, 341.
FAHR, A., HASSANZADEH, P., and ATKINSON, D. B., 1998, *Chem. Phys. Lett.*, **236**, 43.
GRANGEON, F., MONARD, C., DORIER, J.-L., HOWLING, A. A., HOLLENSTEIN, CH., ROMANINI, D., and SADEGHI, N., 1999, *Plasma Sources Sci. Technol.*, **8**, 448.
HAHN, J. W., YOO, Y. S., LEE, J. Y., KIM, J. W., and LEE, H.-W., 1999, *Appl. Optics*, **38**, 1859.
HE, Y., HIPPLER, M., and QUACK, M., 1998, *Chem. Phys. Lett.*, **289**, 527.
HE, Y., and ORR, B. J., 2000, *Chem. Phys. Lett.*, **319**, 131.
HEMMERLING, B., and KOZLOV, D. N., 1999, *Appl. Optics*, **38**, 1001.
HERBELIN, J. M., MCKAY, J. A., KWOK, M. A., UEUNTEN, R. H., UREVIG, D. S., SPENCER, D. J., and BENARD, D. J., 1980, *Appl. Optics*, **19**, 144.
HIPPLER, M., and QUACK, M., 1999, *Chem. Phys. Lett.*, **314**, 273.
HODGES, J. T., LOONEY, J. P., and VAN ZEE, R. D., 1996a, *Appl. Optics*, **35**, 4112; 1996b, *J. chem. Phys.*, **105**, 10278.
HOWIE, W. H., LANE, I. C., NEWMAN, S. M., JOHNSON, D. A., and ORR-EWING, A. J., 1999, *Phys. Chem. chem. Phys.*, **1**, 3079.
HUESTIS, D. L., COPELAND, R. A., KNUTSEN, K., SLANGER, T. G., JONGMA, R. T., BOOGAARTS, M. G. H., and MEIJER, G., 1994, *Can. J. Phys.*, **72**, 1109.
INBAR, E., and ARIE, A., 1999, *Appl. Phys.* B, **68**, 99.
ITO, F., and NAKANAGA, T., 2000, *Chem. Phys. Lett.*, **318**, 571.
JACOB, D., BRETENAKER, F., POURCELOT, P., RIO, P., DUMONT, M., and DORÉ, A., 1994, *Appl. Optics*, **33**, 3175.
JONGMA, R. T., BOOGAARTS, M. G. H., HOLLEMAN, I., and MEIJER, G., 1995, *Rev. scient. Instrum.*, **66**, 2821.
JONGMA, R. T., BOOGAARTS, M. G. H., and MEIJER, G., 1994, *J. molec. Spectrosc.*, **165**, 303.

Kastler, A., 1974, *Nouv. Rev. Optique*, **5**, 133.
King, M. D., Dick, E. M., and Simpson, W. R., 2000, *Atmos. Environment*, **34**, 685.
Kleine, D., Stry, S., Lauterbach, J., Kleinermanns, K., and Hering, P., 1999, *Chem. Phys. Lett.*, **312**, 185.
Kotterer, M., Conceicao, J., and Maier, J. P., 1996, *Chem. Phys. Lett.*, **259**, 233.
Kotterer, M., and Maier, J. P., 1997, *Chem. Phys. Lett.*, **266**, 342.
Kraus, D., Saykally, R. J., and Bondybey, V. E., 1998, *Chem. Phys. Lett.*, **295**, 285; 1999, *Chem. Phys.*, **247**, 431.
Labazan, I., Rudić, S., and Milošević, S., 2000, *Chem. Phys. Lett.*, **320**, 613.
Le Grand, Y., and Le Floch, A., 1990, *Appl. Optics*, **29**, 1244.
Lehmann, K. K., and Romanini, D., 1996, *J. chem. Phys.*, **105**, 10263.
Lehr, L., and Hering, P., 1997a, *IEEE J. quant. Electron.*, **33**, 1465; 1997b, *Appl. Phys.* B, **65**, 595.
Levenson, M. D., Paldus, B. A., Spence, T. G., Harb, C. C., Harris, J. S. Jr, and Zare, R. N., 1998, *Chem. Phys. Lett.*, **290**, 335.
Levenson, M. D., Paldus, B. A., Spence, T. G., Harb, C. C., Zare, R. N., Lawrence, M. J., and Byer, R. L., 2000, *Optics Lett.*, **25**, 920.
Lin, M. C., and Yu, T., 1993, *Int. J. chem. Kinetics*, **25**, 875.
Linnartz, H., Motylewski, T., and Maier, J. P., 1998, *J. chem. Phys.*, **109**, 3819.
Linnartz, H., Motylewski, T., Vaizert, O., Maier, J. P., Apponi, A. J., McCarthy, M. C., Gottlieb, C. A., and Thaddeus, P., 1999, *J. molec. Spectrosc.*, **197**, 1.
Linnartz, H., Vaizert, O., Motylewski, T., and Maier, J. P., 2000, *J. chem. Phys.*, **112**, 9777.
Liu, K., Dulligan, M., Bezel, I., Kolessov, A., and Wittig, C., 1998, *J. chem. Phys.*, **108**, 9614.
Lommatzsch, U., Wahl, E. H., Owano, T. G., Kruger, C. H., and Zare, R. N., 2000, *Chem. Phys. Lett.*, **320**, 339.
Lozovsky, V. A., Derzy, I., and Cheskis, S., 1998, *Chem. Phys. Lett.*, **284**, 407.
Martin, J., Paldus, B. A., Zalicki, P., Wahl, E. H., Owano, T. G., Harris J. S., Jr, Kruger, C. H., and Zare, R. N., 1996, *Chem. Phys. Lett.*, **258**, 63.
McIlroy, A., 1998, *Chem. Phys. Lett.*, **296**, 151; 1999, *Isr. J. Chem.*, **39**, 55.
Meijer, G., Boogaarts, M. G. H., Jongma, R. T., Parker, D. H., and Wodtke, A. M., 1994, *Chem. Phys. Lett.*, **217**, 112.
Mercier, X., Jamette, P., Pauwels, J. F., and Desgroux, P., 1999a, *Chem. Phys. Lett.*, **305**, 334.
Mercier, X., Therssen, E., Pauwels, J. F., and Desgroux, P., 1999b, *Chem. Phys. Lett.*, **299**, 75.
Miller, G. P., and Winstead, C. B., 1997, *J. Anal. Atom. Spectrosc.*, **12**, 907; 2000, *Encyclopedia of Analytical Chemistry*, edited by R. A. Meyers (New York: Wiley).
Min, Z., Wong, T.-H., Quandt, R., and Bersohn, R., 1999, *J. phys. Chem.* A, **103**, 10451.
Motylewski, T., and Linnartz, H., 1999, *Rev. scient. Instrum.*, **70**, 1305.
Motylewski, T., Vaizert, O., Giesen, T. F., Linnartz, H., and Maier, J. P., 1999, *J. chem. Phys.*, **111**, 6161.
Moule, D. C., Burling, I. R., Liu, H., and Lim, E. C., 1999, *J. chem. Phys.*, **111**, 5027.
Mürtz, M., Frech, B., and Urban, W., 1999, *Appl. Phys.* B, **68**, 243.
Nakagawa, K., Katsuda, T., Shelkovnikov, A. S., De Labachelerie, M., and Ohtsu, M., 1994, *Optics Commun.*, **107**, 369.
Nam, G.-J., Xia, W., Park, J., and Lin, M. C., 2000, *J. phys. Chem.* A, **104**, 1233.
Naus, H., de Lange, A., and Ubachs, W., 1997, *Phys. Rev.* A, **56**, 4755.
Naus, H., Navaian, K., and Ubachs, W., 1999, *Spectrochimica Acta* A, **55**, 1255.
Naus, H., and Ubachs, W., 1999a, *J. molec. Spectrosc.*, **193**, 442; 1999b, *Appl. Optics*, **38**, 3423; 2000, *Optics Lett.*, **25**, 347.
Naus, H., van der Wiel, S. J., and Ubachs, W., 1998, *J. molec. Spectrosc.*, **192**, 162.
Newman, S. M., Howie, W. H., Lane, I. C., Upson, M. R., and Orr-Ewing, A. J., 1998, *J. chem. Soc., Faraday Trans.*, **94**, 2681.
Newman, S. M., Lane, I. C., Orr-Ewing, A. J., Newnham, D. A., and Ballard, J., 1999, *J. chem. Phys.*, **110**, 10749.
Ninomiya, Y., Hashimoto, S., Kawasaki, M., and Wallington, T. J., 2000, *Int. J. chem. Kinetics*, **32**, 125.
O'Keefe, A., 1998, *Chem. Phys. Lett.*, **293**, 331.

O'KEEFE, A., and DEACON, D. A. G., 1988, *Rev. scient. Instrum.*, **59**, 2544.
O'KEEFE, A., SCHERER, J. J., COOKSY, A. L., SHEEKS, R., HEATH, J., and SAYKALLY, R. J., 1990, *Chem. Phys. Lett.*, **172**, 214.
O'KEEFE, A., SCHERER, J. J., PAUL, J. B., 1999, *Chem. Phys. Lett.*, **307**, 343.
PALDUS, B. A., HARB, C. C., SPENCE, T. G., WILKE, B., XIE, J., HARRIS, J. S., and ZARE, R. N., 1998, *J. appl. Phys.*, **83**, 3991.
PALDUS, B. A., HARB, C. C., SPENCE, T. G., ZARE, R. N., GMACHL, C., CAPASSO, F., SIVCO, D. L., BAILLARGEON, J. N., HUTCHINSON, A. L., and CHO, A. Y., 2000, *Optics Lett.*, **25**, 666.
PALDUS, B. A., HARRIS, J. S., JR, MARTIN, J., XIE, J., and ZARE, R. N., 1997, *J. appl. Phys.*, **82**, 3199.
PARK, J., BUROVA, S., RODGERS, A. S., and LIN, M. C., 1999a, *J. phys. Chem.* A, **103**, 9036.
PARK, J., CHAKRABORTY, D., BHUSARI, D. M., and LIN, M. C., 1999b, *J. phys. Chem.* A, **103**, 4002.
PARK, J., GHEYAS, S. I., and LIN, M. C., 1999c, *Int. J. chem. Kinetics*, **31**, 645.
PAUL, J. B., COLLIER, C. P., SAYKALLY, R. J., SCHERER, J. J., O'KEEFE, A., 1997, *J. phys. Chem.* A, **101**, 5211.
PAUL, J. B., PROVENCAL, R. A., CHAPO, C., PETTERSON, A., and SAYKALLY, R. J., 1998a, *J. chem. Phys.*, **109**, 10201.
PAUL, J. B., PROVENCAL, R. A., CHAPO, C., ROTH, K., CASAES, R., and SAYKALLY, R. J., 1999, *J. phys. Chem.* A, **103**, 2972.
PAUL, J. B., PROVENCAL, R. A., and SAYKALLY, R. J., 1998b, *J. phys. Chem.* A, **102**, 3279.
PAUL, J. B., and SAYKALLY, R. J., 1997, *Anal. Chem.*, **69**, 287.
PAUL, J. B., SCHERER, J. J., COLLIER, C. P., and SAYKALLY, R. J., 1996, *J. chem. Phys.*, **104**, 2782.
PEARSON, J., ORR-EWING, A. J., ASHFOLD, M. N. R., and DIXON, R. N., 1996, *J. chem. Soc., Faraday Trans.*, **92**, 1283; 1997, *J. chem. Phys.*, **106**, 5850.
PEETERS, R., BERDEN, G., APITULEY, A., and MEIJER, G., 2000, *Appl. Phys.* B **71**, 217.
PIBEL, C. D., MCILROY, A., TAATJES, C. A., ALFRED, S., PATRICK, K., and HALPERN, J. B., 1999, *J. chem. Phys.*, **110**, 1841.
PIPINO, A. C. R., 1999, *Phys. Rev. Lett.*, **83**, 3093; 2000, *Appl. Optics*, **39**, 1449.
PIPINO, A. C. R., HUDGENS, J. W., and HUIE, R. E., 1997a, *Rev. scient. Instrum.*, **68**, 2978; 1997b, *Chem. Phys. Lett.*, **280**, 104.
POIRSON, J., BRETENAKER, F., VALLET, M., and LE FLOCH, A., 1997, *J. opt. Soc. Am.* B, **14**, 2811.
PROVENCAL, R. A., CASAES, R. N., ROTH, K., PAUL, J. B., CHAPO, C. N., SAYKALLY, R. J., TSCHUMPER, G. S., and SCHAEFER, H. F., III, 2000, *J. phys. Chem.* A, **104**, 1423.
PROVENCAL, R. A., PAUL, J. B., ROTH, K., CHAPO, C., CASAES, R. N., SAYKALLY, R. J., TSCHUMPER, G. S., and SCHAEFER, H. F., III, 1999, *J. chem. Phys.*, **110**, 4258.
PUSHKARSKY, M. B., ZALYUBOVSKY, S. J., and MILLER, T. A., 2000, *J. chem. Phys.*, **112**, 10695.
QUANDT, E., KRAEMER, I., and DÖBELE, H. F., 1998, *Europhys. Lett.*, **45**, 32.
RAMPONI, A. J., MILANOVICH, F. P., KAN, T., and DEACON, D., 1988, *Appl. Optics*, **27**, 4606.
REMPE, G., THOMPSON, R. J., KIMBLE, H. J., and LALEZARI, R., 1992, *Optics Lett.*, **17**, 363.
ROMANINI, D., BIENNIER, L., SALAMA, F., KACHANOV, A., ALLAMANDOLA, L. J., and STOECKEL, F., 1999a, *Chem. Phys. Lett.*, **303**, 165.
ROMANINI, D., DUPRÉ, P., and JOST, R., 1999b, *Vibr. Spectrosc.*, **19**, 93.
ROMANINI, D., KACHANOV, A. A., SADEGHI, N., and STOECKEL, F., 1997a, *Chem. Phys. Lett.*, **264**, 316.
ROMANINI, D., KACHANOV, A. A., and STOECKEL, F., 1997b, *Chem. Phys. Lett.*, **270**, 538; 1997c, *ibid.* **270**, 546.
ROMANINI, D., and LEHMANN, K. K., 1993, *J. chem. Phys.*, **99**, 6287; 1995, *ibid.*, **102**, 633; 1996a, *ibid.*, **105**, 68; 1996b, *ibid.*, **105**, 81.
RUTH, A. A., FERNHOLZ, T., BRINT, R. P., and MANSFIELD, M. W. D., 1998, *Chem. Phys. Lett.*, **287**, 403.
RUTH, A. A., KIM, E., -K., and HESE, A., 1999, *Phys. Chem. chem. Phys.*, **1**, 5121.
SAPPEY, A. D., HILL, E. S., SETTERSTEN, T., and LINNE, M. A., 1998, *Optics Lett.*, **23**, 954.
SCHERER, J. J., 1998, *Chem. Phys. Lett.*, **292**, 143.
SCHERER, J. J., ANIOLEK, K. W., CERNANSKY, N. P., and RAKESTRAW, D. J., 1997a, *J. chem. Phys.*, **107**, 6196.

SCHERER, J. J., PAUL, J. B., COLLIER, C. P., O'KEEFE, A., and SAYKALLY, R. J., 1995a, *J. chem. Phys.*, **103**, 9187.
SCHERER, J. J., PAUL, J. B., COLLIER, C. P., and SAYKALLY, R. J., 1995b, *J. chem. Phys.*, **102**, 5190; 1995c, *ibid.*, **103**, 113.
SCHERER, J. J., PAUL, J. B., O'KEEFE, A., and SAYKALLY, R. J., 1995d, *Advances in Metal and Semiconductor Clusters*, Vol. 3, edited by M. A. Duncan (JAI Press), p. 149; 1997b, *Chem. Rev.*, **97**, 25.
SCHERER, J. J., PAUL, J. B., and SAYKALLY, R. J., 1995e, *Chem. Phys. Lett.*, **242**, 395.
SCHERER, J. J., and RAKESTRAW, D. J., 1997, *Chem. Phys. Lett.*, **265**, 169.
SCHERER, J. J., VOELKEL, D., and RAKESTRAW, D. J., 1997c, *Appl. Phys.* B, **64**, 699.
SCHERER, J. J., VOELKEL, D., RAKESTRAW, D. J., PAUL, J. B., COLLIER, C. P., SAYKALLY, R. J., and O'KEEFE, A., 1995f, *Chem. Phys. Lett.*, **245**, 273.
SCHULZ, K. J., and SIMPSON, W. R., 1998, *Chem. Phys. Lett.*, **297**, 523.
SEISER, N., and ROBIE, D. C., 1998, *Chem. Phys. Lett.*, **282**, 263.
SLANGER, T. G., HUESTIS, D. L., COSBY, P. C., NAUS, H., and MEIJER, G., 1996, *J. chem. Phys.*, **105**, 9393.
SPAANJAARS, J. J. L., TER MEULEN, J. J., and MEIJER, G., 1997, *J. chem. Phys.*, **107**, 2242.
SPENCE, T. G., HARB, C. C., PALDUS, B. A., ZARE, R. N., WILLKE, B., and BYER, R. L., 2000, *Rev. scient. Instrum.*, **71**, 347.
SPULER, S., LINNE, M., SAPPEY, A., and SNYDER, S., 2000, *Appl. Optics*, **39**, 2480.
STOLK, R. L., and TER MEULEN, J. J., 1999, *Diamond Relat. Mater.*, **8**, 1251.
TAO, S., MAZZOTTI, F. J., WINSTEAD, C. B., and MILLER, G. P., 2000, *Analyst*, **125**, 1021.
THOMAN, J. W., and MCILROY, A., 2000, *J. phys. Chem.* A, **104**, 4953.
TONOKURA, K., MARUI, S., and KOSHI, M., 1999, *Chem. Phys. Lett.*, **313**, 771.
TOTSCHNIG, G., BAER, D. S., WANG, J., WINTER, F., HOFBAUER, H., and HANSON, R. K., 2000, *Appl. Optics*, **39**, 2009.
VANDER WAL, R. L., and TICICH, T. M., 1999, *Appl. Optics*, **38**, 1444.
VAN DE SANDEN, M. C. M., VAN HEST, M. F. A. M., DE GRAAF, A., SMETS, A. H. M., LETOURNEUR, K. G. Y., BOOGAARTS, M. G. H., and SCHRAM, D. C., 1999, *Diamond Relat. Mater.*, **8**, 677.
VAN ZEE, R. D., HODGES, J. T., and LOONEY, J. P., 1999, *Appl. Optics*, **38**, 3951.
VASUDEV, R., USACHEV, A., and DUNSFORD, W. R., 1999, *Environmental Sci. Technol.*, **33**, 1936.
WAHL, E. H., OWANO, T. G., KRUGER, C. H., MA, Y., ZALICKI, P., and ZARE, R. N., 1997, *Diamond Relat. Mater.*, **6**, 476.
WAHL, E. H., OWANO, T. G., KRUGER, C. H., ZALICKI, P., MA, Y., and ZARE, R. N., 1996, *Diamond Relat. Mater.*, **5**, 373.
WHEELER, M. D., NEWMAN, S. M., ISHIWATA, T., KAWASAKI, M., and ORR-EWING, A. J., 1998a, *Chem. Phys. Lett.*, **285**, 346.
WHEELER, M. D., NEWMAN, S. M., and ORR-EWING, A. J., 1998b, *J. chem. Phys.*, **108**, 6594.
WHEELER, M. D., NEWMAN, S. M., ORR-EWING, A. J., and ASHFOLD, M. N. R., 1998c, *J. chem. Soc., Faraday Trans.*, **94**, 337.
WHEELER, M. D., ORR-EWING, A. J., and ASHFOLD, M. N. R., 1997a, *J. chem. Phys.*, **107**, 7591.
WHEELER, M. D., ORR-EWING, A. J., ASHFOLD, M. N. R., and ISHIWATA, T., 1997b, *Chem. Phys. Lett.*, **268**, 421.
WINSTEAD, C. B., MAZZOTTI, F. J., MIERZWA, J., and MILLER, G. P., 1999, *Anal. Commun.*, **36**, 277.
XIE, J., PALDUS, B. A., WAHL, E. H., MARTIN, J., OWANO, T. G., KRUGER, C. H., HARRIS, J. S., and ZARE, R. N., 1998, *Chem. Phys. Lett.*, **284**, 387.
XU, S., DAI, D., XIE, J., SHA, G., and ZHANG, C., 1999, *Chem. Phys. Lett.*, **303**, 171.
YE, J., and HALL, J. L., 2000, *Phys. Rev.* A, **61**, 061802(R).
YE, J., MA, L.-S., and HALL, J. L., 1998, *J. opt. Soc. Am.* B, **15**, 6.
YU, T., and LIN, M. C., 1993, *J. Am. chem. Soc.*, **115**, 4731; 1994a, *J. phys. Chem.*, **98**, 2105; 1994b, *J. Am. chem. Soc.*, **116**, 9571; 1994c, *J. phys. Chem.*, **98**, 9697; 1994d, *Int. J. chem. Kinetics*, **26**, 771; 1995a, *Combust. Flame*, **100**, 169; 1995b, *J. phys. Chem.* **99**, 8599.
YU, T., MEBEL, A. M., and LIN, M. C., 1995, *J. phys. org. Chem.*, **8**, 47.
ZALICKI, P., MA, Y., ZARE, R. N., WAHL, E. H., DADAMIO, J. R., OWANO, T. G., and KRUGER, C. H., 1995a, *Chem. Phys. Lett.*, **234**, 269.

ZALICKI, P., MA, Y., ZARE, R. N., WAHL, E. H., OWANO, T. G., and KRUGER, C. H., 1995b, *Appl. Phys. Lett.*, **67**, 144.
ZALICKI, P., and ZARE, R. N., 1995, *J. chem. Phys.*, **102**, 2708.
ZHAO, M., WAHL, E. H., OWANO, T. G., LARGENT, C. C., ZARE, R. N., and KRUGER, C. H., 2000, *Chem. Phys. Lett.*, **318**, 555.
ZHU, L., and CRONIN, T. J., 2000, *Chem. Phys. Lett.*, **317**, 227.
ZHU, L., CRONIN, T., and NARANG, A., 1999, *J. phys. Chem.* A, **103**, 7248.
ZHU, L., and DING, C.-F., 1997, *Chem. Phys. Lett.*, **265**, 177.
ZHU, L., and JOHNSTON, G., 1995, *J. phys. Chem.*, **99**, 15114.
ZHU, L., and KELLIS, D., 1997, *Chem. Phys. Lett.*, **278**, 41.
ZHU, L., KELLIS, D., and DING, C-F., 1996, *Chem. Phys. Lett.*, **257**, 487.